Evolution of tonoplast P-ATPase transporters involved in vacuolar acidification

Evolution of tonoplast P-ATPase transporters involved in vacuolar hyperacidification

Sofia Provenzano[a,c,1], Mattijs Bliek[a,b,1], Cornelis Spelt[a,b,1,] Yanbang Li[a,b], Laura Machado de Faria[a,3], Ingo Appelhagen[c,4], Walter Verweij[a,5], Andrea Schubert[d], Martin Sagasser[c], Bernd Weisshaar[c], Ronald Koes[a,b,2] and Francesca Quattrocchio[a,b,2].

[a]Department of Molecular and Cell Biology, VU-University, De Boelelaan 1081, 1071HK Amsterdam, The Netherlands.

[b]Swammerdam Institute for Life Sciences, University of Amsterdam, Amsterdam, The Netherlands. [c]Genome Research, Faculty of Biology, Bielefeld University, Universitaetstrasse 27, 33615 Bielefeld, Germany

[d]Department of Agricultural, Forestry and Food Sciences, University of Turin, 10095 Grugliasco, Italy.

[e]Genome Research, Faculty of Biology, Bielefeld University, Universitaetstrasse 27, 33615 Bielefeld, Germany

Running Title: Evolution of tonoplast P-ATPases.

Keywords: P-ATPase | proton pump | evolution | vacuolar hyperacidification |horizontal gene transfer

Footnotes

[1]S.P., M.B and K.S. equally contributed to this work

[2]To whom correspondence may be addressed. Email: f.m.quattrocchio@vu.nl or ronald.koes@vu.nl; Regular mail: Department of Molecular and Cell Biology, VU-University, De Boelelaan 1081, 1071HK Amsterdam, The Netherlands

[3]Present address: Federal University of Rio de Janeiro - UFRJ, Institute of Biophysics Carlos Chagas Filho, Laboratory of Modeling and Molecular Dynamics, Rio de Janeiro, Brazil.

[4]Present address: John Innes Centre, Department of Metabolic Biology, Norwich Research Park, Norwich NR4 7UH, United Kingdom

[5]Present address: The Genome Analysis Centre (TGAC), Norwich Research Park, Norwich, NR4 7UH,UK Norwich.

The authors responsible for distribution of materials integral to the findings presented in this article in accordance with the policy described in the Instructions for Authors (www.plantcell.org) are: F.Quattrocchio (f.m.quattrocchio@vu.nl), and Ronald Koes (ronald.koes@vu.nl).

ABSTRACT

Petunia mutants with blue flowers uncovered a novel proton pump that controls the pH of the central vacuole in the pigmented petal epidermal cells.. The components of this pump are two interacting P-ATPase, PH1 and PH5, residing in the vacuolar membrane (tonoplast). PH5 has high similarity to plasma membrane proton pumps from the P_{3A}-ATPase family, whereas PH1 is the only known eukaryotic member of the P_{3B}-ATPAse family. As there are no indications that such a pump might operate in other species, we investigated the distribution and evolution of PH1 and PH5 homologs in the plant kingdom. Mining of databases and complementation experiments revealed that (functional) PH1 and PH5 homologs are widespread among angiosperms. Phylogenetic analysis suggests that PH5 originated from plasma membrane proton transporters by the acquisition of a new subcellular localization and new regulation mechanism. PH1 shares its origins with bacterial magnesium transporters, suggesting horizontal transfer either from bacteria to plants or vice versa. PH1 is irregularly distributed within plant families, possibly due to repeated loss. The wide conservation of PH1 and PH5 homologs, also in species lacking colored insect-pollinated flowers, suggests that these genes are involved in other phenomena requiring strong(er) vacuolar acidification, and perhaps other endomembrane compartments.

INTRODUCTION

In plant cells the vacuole is the biggest compartment and can in same cases occupy over 90% of the cell volume. The lumen of this organelle is used for the storage of different molecules, ranging from proteins to sugars, ions, and a variety of secondary metabolites (Taiz, 1992). The transport of molecules in and out of the vacuole is for large part depending on the pH gradient across its membrane (tonoplast). This proton gradient energizes a plethora of transporters, which exchange protons (transported down their gradient) for other molecules (transported against their gradient)(Nelson et al., 2000; Beyenbach and Wieczorek, 2006). The acidification of the vacuolar lumen also controls the activity of several enzymes residing in this organelle. In most cells the activity of a (nearly) ubiquitous V-ATPase proton pump generates a mildly acidic lumen of the vacuole and other compartments. V-ATPases probably originated from mitochondrial F0-F1-ATPase and are evolutionary very old because they are found in

all kingdoms of life (Gaxiola et al., 2007; Schumacher and Krebs, 2010). Plants and some sporadic protists, bacteria and Archea posses an additional pyrophosphatase (PPase) proton pump (Drozdowicz and Rea, 2001), which is presumably less powerful than a V-ATPase (Rea and Sanders, 1987). However in specialized cell types vacuoles can be very acidic and display a much larger proton gradient, An extreme example are lemon fruit juice cells, in which the vacuolar lumen has a pH around 2 (Muller and Taiz, 2002). In petals of petunia, vacuoles are also hyperacidified, albeit much less extremely, which result in a reddish flower color that is important for the attraction of pollinating animals.

The pigmentation of flowers, fruits and foliage, is due to the accumulation of anthocyanin pigments in the central vacuole of (sub)epidermal cells (Koes et al., 2005). The color of these tissues depends on multiple factors, including vacuolar pH (Koes et al., 2005), as the absorption spectrum of anthocyanins depends on the pH of the solvent (Yazaki, 1976). In petunia, a group of transcription factors has been shown to regulate both anthocyanin accumulation and acidification of the vacuole in cells of the epidermis of flower petals. Among these regulators, is (AN1), a bHLH transcription factor that can interact with one partner of the MYB family (AN2) forming a transcription complex able to activate anthocyanin biosynthetic genes, or with a second MYB partner (PH4) to activate genes involved in vacuolar acidification (Spelt et al., 2002). PH4 and AN1 work in conjunction with the transcription factors PH3 and AN11, which also promote anthocyanin biosynthesis (Spelt et al., 2002; Quattrocchio et al., 2006). Among the target genes of these regulators are *PH1* and *PH5*, which encode P-ATPase ion pumps that are essential for vacuolar hyperacidification which affect the final color of pigments conferring a reddish flower color (Verweij et al., 2008; Faraco, 2011). In mutants affecting any of the components of the pathway leading to vacuolar acidification, flowers get a bluish color and the pH of the petal extracts is higher than that of wild type siblings.

P-type ATPases constitute a large superfamily of ATP-powered ion pumps found in eukaryotes, Archaea and bacteria, which can be divided in 5 families (P1 to P5) of transporters that translocate different ions (Duby and Boutry, 2009; Palmgren and Nissen, 2011). PH5 belongs to the P_{3A}-ATPase family of proton pumps found in fungi and plants (Verweij et al., 2008,). The genomes of yeast and primitive plants (algae, bryophyte, lycophyte) encode some 2 or 3 P_{3A}-ATPases (Ulaszewski et al., 1983; Pedersen et al., 2012) In higher plants this family expanded to some 10-15

proteins, which group in 5 subgroups (I to V) of 1-3 proteins each (Arango et al., 2003; Baxter et al., 2003; Pedersen et al., 2012). P_{3A}-ATPases of Arabidopsis and/ or *Nicotiana plumbaginifolia* belonging to groups I, II and IV reside in the plasma membrane (PM) (DeWitt and Sussman, 1995; DeWitt et al., 1996; Kim et al., 2001; Lefebvre et al., 2004; Lefebvre et al., 2005) and are important to energize various PM-based transporters and to regulate cytoplasmic pH (Palmgren, 2001). PH5 of petunia, which is most similar to type III proteins, is instead localized on the tonoplast and is required for the hyperacidification of the vacuolar lumen (Verweij et al., 2008; Faraco et al., 2014). How PH5 acquired this distinct intracellular localization during evolution and whether that is conserved is currently unknown. The Arabidopsis P_{3A}-ATPase with most similarity to PH5 is At AHA10. AHA10 is, like PH5, required for proanthocyanin accumulation in the seed coat (Baxter et al., 2005), but its mode of action, intracellular localization and phylogenetic relationship to PH5 has remained unclear.

PH1 belongs to the distinct subfamily of P_{3B}-ATPases (Faraco et al., 2014), which was thought to be unique for prokaryotes (Smith and Maguire, 1998a). Bacterial P_{3B}-ATPases, like MgtA from *E. coli*, were discovered as facilitators of Mg^{2+} import, although that is unlikely to be their primary function (Smith and Maguire, 1998b), whereas the ion pumped by PH1 in plant cells (if any) is unknown (Faraco et al., 2014). PH1 can interact with PH5 to boost H^+ pumping activity and ectopic co-expression of PH1 and PH5, for example in leaves, lowers the pH in these tissues (Faraco et al., 2014), demonstrating that these two P-ATPases acidify vacuoles further than the ubiquitous V-ATPase and PPase pumps. Interestingly, the combined expression of PH1 and PH5 results in suppression of the activity of the V-ATPase, indicating that the hyperacidifcation of the vacuoles is driven by P-ATPase activity alone (Faraco et al., 2014).

Over decades, or even centuries, breeders and geneticists collected a wealth of pigmentation mutants in a wide range of species. With few exceptions these mutations concern defects in conserved anthocyanin biosynthetic genes. Surprisingly, *ph* mutants were found only in petunia. In addition, electrophysiological studies in a multitude of species also did not uncover evidence for tonoplast pumps related to PH1 and PH5. This raises the question whether the PH1/PH5 acidification pathway is of general interest or an eccentric feature of a few species only.

Here, we show that homologs of PH1 and PH5 are wide spread among angiosperms and that homologs of divergent dicots are functionally interchangeable. Phylogenetic and functional evidence indicates that PH5 homologs originated by vertical transfer from plasma membrane P_{3A}-ATPases prior to the appearance of angiosperms, and that alterations in the cytoplasmic C- and N-terminal domains changed the intracellular localization and interactions with other (regulatory) proteins. The evolution of PH1 on the other hand is more complex. The distribution of PH1 in different plant families indicates that it could have been acquired by one or more events of horizontal transfer followed by numerous events of loss. The presence of both PH1 and PH5 in the genomes of divergent plant species indicates functions of these two pumps in tissues other than brightly colored petals.

RESULTS

PH5 homologs from different species.

To understand how PH5 evolved acquired its vacuolar localization we searched GenBank, Phytozome and various dedicated databases, which yielded sequences of P_{3A}-ATPases from a range of species. In addition a (putative) PH5-homolog from rose (*Rosa hybrida*, Rh PH5) was isolated by hybridization of a rose petal cDNA library. Using primers complementary to specifically conserved region in Rh *PH5* and Ph *PH5* we amplified by PCR a potential *PH5* homolog (Dc PH5) from cDNA prepared from petals of carnation (*Dianthus caryophyllus*). P_{3A}-ATPases of different species and clades display high similarity throughout the protein (Figure 1A). Phylogenetic analysis shows that PH5 homologs from petunia (Ph PH5) Arabidopsis (At AHA10), grape (Vv PH5), carnation (Dc PH5) and other seed plants constitute a well-defined clade within the P_{3A}-ATPase family (Figure 2A). The common origin of these putative *PH5* homologs is supported by their similar intron/exon architecture. The *PH5* homologs from dicots all contain 21 exons separated by introns in identical positions (Figure 1B), although the size and sequence of these introns is completely different. The *PH5* homologs from the monocots rice (Os *AHA9*) and *Setaria italica* (*Si034109m.g*) have a similar architecture as the dicot genes except that they lack one intron (intron 13). P_{3A}-ATPase genes from different species which group in distinct subclades, contain distinct subsets of the same introns found in PH5 homologs (Figure

1B) (Arango et al., 2003). This indicates that introns have been gained or lost multiple times in the distinct branches of the P_{3A}-ATPase gene family.

Functional characterization of PH5 homologs.

To analyze whether PH5 homologs from different species are functionally interchangeable, we expressed PH5 homologs from carnation, rose, grape and Arabidopsis from the p35S promoter in a petunia *ph5* mutant. We generated for each construct 15 to 20 transgenic plants. All tested PH5 homologs, as well as the Rh PH5-GFP fusion, were able to complement the mutant *ph5* phenotype and to restore both the flower color and the pH of the crude petal extracts in about 50% of the transgenic plants (Figure 3A). Supplemental Figure 1 online shows that all complemented transgenic plants express the transgene. In addition, we generated 25 *ph5* transformants containing *p35S:*At *AHA2*. Although several of these plants expressed the transgene at a similar level as the transformants complemented by PH5 homologs (Supplemental Figure 1 online), none of them showed rescue of the *ph5* phenotype (Figure 3A).

Because the feature that distinguishes Ph PH5 from previously characterized P_{3A}-ATPases is its vacuolar localization, we hypothesized that functionally interchangeable P_{3A}-ATPases also reside in the tonoplast, whereas other P_{3A}-ATPases reside elsewhere. To test this idea we transformed petunia petal protoplasts with constructs expressing GFP-fusions of different P_{3A}-ATPases together with a construct expressing AtSYP122-RFP, which marks the plasma membrane of transformed cells. Ph PH5-GFP was visible on the tonoplast 48 hours after transformation (Figure 3B), consistent with previous results (Verweij et al., 2008). Expression of At AHA10, Vv PH5, Dc PH5 and Rh PH5 gave the same results, whereas At AHA2-GFP and the petunia homolog Ph AHA2-GFP both localized to the plasma membrane (Figure 3B).

The complementation of *ph5* by *p35S:*Rh *PH5-GFP* (Figure 3A) is on its own an unreliable measure for the fidelity of this GFP fusion (Quattrocchio et al., 2013). More importantly, we found that the Rh PH5-GFP accumulating in transgenic petals is full size, and no cleavage products were observed (Figure 3C). This implies that the fluorescence reproduces the localization of the intact fusion protein and not that of aberrant cleavage products (Quattrocchio et al., 2013).

These results indicate that PH5 homologs are tonoplast-localized proteins and that distinct P_{3A}-ATPases like AtAHA2, which are also proton transporters, cannot

replace PH5 because they reside elsewhere. This implies that the acquisition of new signals for sorting to the vacuole must have been a crucial step in the divergence of PH5 homologs from plasma membrane P_{3A}-ATPases

Proteins of the PH5 clade evolved from plasma membrane ATPases by limited changes in their termini.

PH5-homologs and other P_{3A}-ATPases (including those residing in the plasma membrane) display high similarity over almost their entire length (Figure 1). However, the two terminal domains, which are cytoplasmic (Arango et al., 2003; Pedersen et al., 2007), differ considerably between the plasma membrane P_{3A}-ATPases (subfamilies I and II) and PH5 homologs (subfamily III) (Figure 4A and B). To examine whether these differences contributed to their distinct cellular localization, we generated constructs for the expression of GFP fusions of PhAHA2 (PhAHA2-GFP), the apparent petunia homolog of the type II protein AHA2 from Arabidopsis, and of a chimera (^{N}PH5-PhAHA2-^{C}PH5-GFP), in which the N- and C-terminal domains of Ph AHA2 were replaced by the equivalent domains from PH5 (Figure 5A). We transformed these constructs in petunia petal protoplasts in combination with the marker for the plasma membrane RFP-AtSYP122 (Assaad et al., 2004). The Ph AHA2-GFP protein marked the circumference of the cells and co-localized with RFP-AtSYP122, indicating that Ph AHA2 resides in the plasma membrane, like AtAHA2 (Figure 5B). By contrast, ^{N}PH5-Ph AHA2-^{C}PH5-GFP instead marked the circumference of the colored vacuole rather than the cell (Figure 5B second row) and does not (co-)localize with RFP-ATSYP122 in the plasma membrane, but in the adjacent vacuolar membrane (Figure 5B third row and insert there in). These results indicate that changes in the sequence of the terminal domains of a plasma membrane P_{3A}-ATPases are sufficient for the acquisition of tonoplast localization.

Alignment of the sequence in the very first portion of the cytoplasmic N-terminal domain of PH5-homologs with the same region of plasma membrane based from groups I and II reveals an insertion of 8 amino acids in the tonoplast proteins (Figures 4A). To examine the importance of these 8 amino acids for targeting of AHA10 to the tonoplast, we generated mutants of the AHA10-GFP fusion protein in which these 8 amino acids were deleted (AHA10$^{\Delta 3\text{-}10}$-GFP) or replaced with alanine

residues (AHA10$^{3\text{-}10>Ala}$-GFP) and a third construct (AHA10$^{8\text{-}10>Ala}$-GFP) in which only the last three residues were substituted by alanine (Figure 6A). We expressed these constructs in tobacco BY2 protoplasts and found that all three mutations affected the tonoplast localization of AHA10. Comparison of the bright field and fluorescence micrograhs (Figure 5B) shows that in BY2 cells free GFP localizes in the cytoplasm, in between the invaginations of the huge vacuole, and in the nucleus, as expected and AHA2-GFP in the outer plasma membrane, whereas both AHA10-GFP and PH5-GFP mark the tonoplast that surrounds the vacuolar invaginations (Figure 6B). The GFP signal for AHA10$^{\Delta 3\text{-}10}$-GFP and AHA10$^{3\text{-}10>Ala}$-GFP marks instead the outer contour of the cell, similar to AHA2-GFP, although some diffuse fluorescence is visible (Figure 6B). AHA10$^{8\text{-}10>Ala}$-GFP gives diffused fluorescence and some plasma membrane localization. This could be due to (partial) instability of the fusion. Altogether these results show that the 8 amino acid motif present in the N-terminal cytoplasmic domain of AHA10 is required for tonoplast localization. PH5 homologs from other species than petunia and Arabidopsis have similar cytoplasmic N-terminal domains, indicating that this is a characteristic acquired when the PH5 ancestor diversified from the other members of the P_{3A}-ATPase family (Figure 4A).

The plasma membrane based P_{3A}-ATPases contain an (auto)inhibitory C-terminal domain, which is regulated by phosphorylation and binding of 14-3-3 proteins. In proteins from the At AHA2 clade (type II) the C-terminus consists of a conserved HYTV motif, and in those from the AtAHA4 clade (type I) a conserved SYTV or AYTV (Figure 4B). Phosphorylation of the penultimate threonine (T) enables the binding to 14-3-3 proteins and the formation of an active hexameric P-ATPase complex (Jahn et al., 1997; Fuglsang et al., 1999; Svennelid et al., 1999; Maudoux et al., 2000; Kanczewska et al., 2005; Ottmann et al., 2007).

In PH5 homologs this motif is replaced by a sequence that lacks the antepenultimate tyrosine residue. In PH5 homologs from dicots the C-terminal motif is AHTV and in the monocots *Oryza sativa* (rice) and *Setaria italica* it is AQTV. Interestingly, the C-terminal sequence of PH5 homolog from the gymnosperm *Picea abies* still contains the antepenultimate tyrosine (AYTV, Figure 4B). This observation supports the origin of PH5 from other P_{3A}-ATPases and indicates that the C-termini of PH5-like proteins differentiated after the separation of gymnosperms from angiosperms.

Because deletion of the YTV motif from At AHA2 abolished 14-3-3 binding and the replacement of any of the three ultimate amino acids (Y, T or V) with alanine severely reduces enzyme activity (Fuglsang et al., 1999), we asked whether the sequence divergence in the C-terminal domain of PH5 homologs affects their interaction with 14-3-3 proteins. We used a yeast two-hybrid (Y2H) assay, which is essentially similar to those used previously to study the interaction of 14-3-3 proteins with Type I and II P_{3A}-ATPases (Jahn et al., 1997; Fuglsang et al., 1999). We found that the C-terminal domain of At AHA2 and Ph AHA2 can interact with 14-3-3 proteins whereas *Ph* PH5 cannot (Figure 7). By contrast, the PH5 C-terminal domain can interact, albeit weakly, with a putative AAA-ATPase (ATPases Associated with diverse cellular Activities) (Iyer et al., 2004) that we identified in a Y2H cDNA library screen, whereas At AHA2 and Ph AHA2 cannot (Figure 7). These results suggest that the divergence of the C-terminal motif of Ph PH5, which is a reliable signature of type III proteins, altered the interactions with other proteins. This suggests that post-translational regulation of PH5 homologs differs from type I and type II proteins and probably does not involve the interaction with 14-3-3 proteins.

Identification of functionally interchangeable PH1 homologs from grape and rose

P_{3B}-ATPases, such as MgtA from *E. coli* and *Salmonella,* were discovered for their involvement in magnesium uptake and were long thought to be specific for prokaryotes (Smith and Maguire, 1998a; Kuhlbrandt, 2004). Database searches with the cDNA sequence of *PH1* uncovered a putative grape homolog (Vv PH1), and PCR amplification, using primers complementary to regions conserved in *PH1* and *Vv PH1*, identified a similar gene from rose (*Rh PH1*). The Vv PH1 and Rh PH1 proteins display high (70%) amino acid similarity with Ph PH1 and conservation of the two cation-binding domains (Supplemental Figure 2 online). The intron/exon structure of the encoding genes is also conserved (Supplemental Figure 2 online). That is, the coding sequences are interrupted by seven introns in the same positions, but the size and sequence of these introns are highly divergent. Although P_{3B}-ATPases are thought to be most related to P_{3A}-ATPases (Axelsen and Palmgren, 1998), the intron/exon organization of the P_{3B} and P_{3A}-ATPase genes is rather different.

To examine whether Vv PH1 and Rh PH1 share functional similarity with PH1, we transformed *p35S*:Ph *PH1*, p35S:Vv *PH1* and p35S:Rh *PH1* constructs in

ph1 petunia plants. As a host we used an F1 hybrid (V23xR170) of two *ph1* mutant lines containing a stable recessive and a weakly unstable *ph1* allele with a transposon insertion, respectively (Faraco et al., 2014). For each construct we obtained about 20 transgenic plants, half of which showed a complemented petal color phenotype. As expected the transposon insertion in the *ph1* allele was retained in all transformants. The best expressors (Supplemental Figure 1 online) produced petals with a red-violet color and a low pH of the crude petal extract as compared to untransformed control plants, which have petals with a blue-violet color and higher pH values (Figure 8A). These results indicate that PH1 is functionally conserved in asterids (petunia) and distantly related rosids (grape and rose), which are the two major clades of dicots.

Distribution of PH1 homologs in the tree of life

To assess the distribution of P_{3A}-ATPases in eukaryotes in further depth, we mined Genbank, Phytozome and various dedicated databases for specific species. We analyzed both predicted protein sequences and entire (translated) genome sequences, as we noticed that PH1 homologs were often overlooked in (early) automated genome annotations. We found putative *PH1* homologs in the genomes of a broad range of angiosperms, including numerous dicot species and three monocots (the date palm *Phoenix dactylifera,* the duckweed *Spirodelq polyrhiza* and the wild banana *Musa acuminata* (Figure 8B and Figure 9). Furthermore we found genes encoding PH1-like proteins in several slime molds, including multiple *Dictyostelium* species and *Polysphondilium pallidum,* and in a few classes of fungi. However, genomes of all metazoans and most fungi, including for example all true yeasts, lack genes that encode PH1-related proteins. As expected we found protein related to PH1/MgtA in some specific groups of bacteria (*Firmucutes* and *Proteobacteria*), and also in Archea (species belonging to the phyla *Euryarchaeota* and *Crenarchaeota*). However, there are also many bacteria and Archea that lack putative PH1/MgtA homologs.

Phylogenetic analysis showed that the P_{3B}-ATPases from bacteria, Archaea and angiosperms constitute a clade that is clearly separate from other P-ATPases and consists of several sister groups roughly comprising (with few exceptions, see Discussion) the plant, fungal, slime mold and prokaryotic proteins respectively (Figure 8B, Supplemental Figures 3 and 4 online). Interestingly, several angiosperm genomes lack PH1-related sequences. For instance, the genomes of several *Brassicaceae* lack P_{3B}-ATPase sequences, as the encoded proteins with most

similarity belong to distinct P-ATPase families. The same holds true for tomato (*Solanum lycopersicum*), potato (*S. tuberosum*) (Figure 8B and Figure 9) and pepper (*C. annuum*, Figure 9). The absence of PH1 homologs in these species seems due to at least two independent losses of *PH1*, as related groups and species do contain a *PH1* homolog (Figure 9). In *S. lycopersicum* the loss of PH1 is associated with deletion of part of a neighboring gene and in *S. tuberosum* with the complete loss of that gene (gene #7 in Figure 10). Also in *Arabidopsis thaliana* and *Capsella rubella* (both *Brassicaceae*), additional genes seem to be missing around the position where *PH1* is located in relatively closely related species. As the "gap" is identical in *Capsella rubella* and *Arabidopsis thaliana*, the loss of PH1 was most likely a single event in a common ancestor of the two species. Additional losses of PH1 may have occurred also within Caryophyllales, because PCR reaction with primers that amplified PH1 homologs from various species did not yield any *bona fide* amplification products from carnation. The genomes of grasses (*Gramineae*) sequenced so far (*Sorghum*, *Panicum*, rice, maize, *Brachypodium*) also lack *PH1*. This seems due to yet another deletion event, as PH1 is present in the genome of other monocots (*Phoenix dactylifera, Spirodela polyrhiza, Musa acuminata*). The absence of PH1 homologs from most of the early sequenced plant genomes (e.g. Arabidopsis) may have contributed to the (wrong) idea that only bacteria had this class of P-ATPases.

To trace the evolutionary origin of the angiosperm PH1 homologs we examined sequences from plant species that are ancestral to monocots and dicots. Among early angiosperms we found a partial EST sequence from the Magnoliid *Persea americana* (avocado) and a complete (predicted) gene from *Amborella trichopoda*. In addition we found a partial sequence of a PH1 related gene in an incomplete genome scaffold of the gymnosperm *Picea abies (*spruce). Phylogenetic analyses indicated that the *Persea*, *Amborella* and *Picea* sequences are more similar, and apparently ancestral, to the angiosperm PH1 homologs (Figure 8B and Supplemental Figure 3 online). Surprisingly, the genomes of more primitive plants, such as the bryophyte *Physcomitrella patens*, the lycophyte *Selaginella moellendorfii*, and the five algae that are represented in Phytozome (*Chlamydomonas reinhardtii, Volvox carteri, Coccomyxa subellipsoidea, Micromonas pusilla and Ostreococcus lucimarinus*), apparently lack PH1 homologs. The green algae *Chlorella variabilis* is a curious exception as is does encode a PH1-related protein. The relationship of this

Chlorella protein with the plant proteins described above is ambiguous. In most of the phylogenetic trees that we generated the *Chlorella* protein clusters with the angiosperm PH1 homologs (Figure 8B and Supplemental Figure 3 online). However, support for this clustering is relatively weak, and a small changes in the selection of proteins used as input (which does affect the curation of the sequence alignment), can strongly decrease the bootstrap support or completely disrupt clustering with the other plant proteins (Figure 8B and Supplemental Figures 3 and 4 online), and in some cases even result in weakly supported clustering of the *Chlorella* protein with fungal P_{3B}-ATPases. Furthermore, the intron-exon architecture of the *Chlorella* gene, which consists of 21 exons, is entirely different from that of the analyzed angiosperms (8 exons in various asterids and rosids and in *Amborella*), fungal (a.o. species with 8 or 13 exons) or slime mold species (2 or 3 exons).

Taken together these data indicate that the angiosperm PH1 homologs derive from a common ancestor that existed already in the earliest angiosperms (the common ancestor of dicots, monocots, magnoliids, and *Amborellales*) and even in (some) gymnosperms. The absence of PH1 homologs in all the primitive species analyzed, except for the algae *C. variabilis*, together with their high similarity to prokaryotic and fungal P_{3B}-ATPases and the scattered distribution of P_{3B}-ATPases among prokaryote and fungal species, are difficult to explain by evolution via vertical transmission and suggests that one or more horizontal gene transfer (HGT) events took place in the (early) evolution of these proteins.

PH1 and PH5 expression in species other than petunia

In petunia the main function of PH1 and PH5 is in the pigmentation of flowers, which is important for the attraction of pollinators, and the accumulation of tannins in the seed (Verweij et al., 2008; Faraco et al., 2014), whereas the role of *AHA10* in Arabidopsis, which has unpigmented self-pollinating flowers, seems limited to the accumulation of tannins in the seed (Baxter et al., 2005). The functional and structural conservation of PH1 and PH5 homologs in the plant kingdom raises questions about their function in species with different flower colors and pollination syndromes. To assess the function of *PH5* and *PH1* homologs, we studied their expression in rose, which produces, like petunia, brightly colored flowers, and grapevine, which has self-pollinating uncolored flowers, but produces colored berries. The grape varieties Barbera and Pinot noir accumulate anthocyanins (mainly malvidin 3-*O* glycosides) in

the skin of the berry starting at *véraison* (the onset of ripening). The berries of Chardonnay are not colored due to mutations in the *MYB* regulators Vv*MYBA1* and Vv*MYBA2,* which are homologs of the petunia anthocyanin regulator *AN2* (Quattrocchio et al., 1999; Kobayashi et al., 2004). We found that Vv *PH5* and Vv *PH1* are expressed in the berry skin of Barbera and Pinot, peaking around *véraison*, (Figure 11 A and B), when anthocyanin biosynthesis starts (Figure 11C). The expression of Vv *PH1,* is much less modulated during fruit development, and its expression is much higher in Barbera than in the other genotypes, while Vv *PH5* is strongly induced during berry development, with the highest expression in berries of Pinot noir (where Vv PH1 is hardly expressed). In the unpigmented Chardonnay berries however, expression of both Vv PH5 and Vv PH1 is lower than in Barbera and Pinot and shows no obvious peak at *véraison*.

In rose Rh *PH5* and Rh *PH1* mRNAs are expressed in petals of developing flower buds and decrease in later stages of development. This temporal expression pattern in rose flowers is coordinated with the accumulation of pigments, which in this species starts very early during the development of the bud (Figure 11). However, Rh *PH1* and Rh *PH5* mRNAs are also detectable in leaves, where usually no pigment accumulates (the leaves used for these experiments showed no pigmentation) (Figure 11D). Rh *PH5* mRNA level in leaves is comparable to that in petals, whereas Rh *PH1* expression in leaves is considerably lower than in petals, These results, although limited to two species, show that PH1 and PH5 could have functions outside petals in both pigmented (e.g. berry) and unpigmented tissues (e.g. rose leaves).

DISCUSSION

Over the centuries a plethora of flower color mutants with defects in anthocyanin has been collected in a wide variety of species, but, curiously mutants such as *ph1* and *ph5* were, to our knowledge only found in petunia, which suggested that the vacuolar pump(s) PH1 and PH5 may be unique to a few species. Here we show that *PH5* and *PH1* homologs existed already in gymnosperms, before flowers made their appearance in evolution, and are today wide spread among angiosperms.

During evolution the P_{3A}-ATPase family expanded from 2-3 genes in algae to five distinct classes in angiosperms that together comprise some 10-15 genes in higher plants. Gene duplicates underwent neo or sub-functionalization. Type I and II

genes diverged by alteration in their transcriptional regulation, as they are expressed today with divergent patterns (Oufattole et al., 2000; Arango et al., 2003)Type III genes, such as *PH5* and *AHA10*, originate from a gene duplication that precedes the appearance of angiosperms and colored flowers. They diverged from the ancestral genes by changes in their expression pattern, and the intracellular localization and post-translational regulation of the encoded proteins. Similar to type I and II proteins (Piotrowski et al., 1998; Axelsen et al., 1999,de Kerchove d'Exaerde, 1995 #2165), PH5 can rescue the growth of a yeast P_{3A}-ATPase mutant, possibly because of (partial) mislocalization to the plasma membrane, indicating that its proton pumping activity is similar to that of type II proteins (Verweij et al., 2008). Hence the finding that in plant cells AHA2 cannot replace the function of PH5, indicates that the acquisition of a tonoplast localization was a key-step for the neo-functionalization of type III proteins.

In plasma membrane P_{3A}-ATPases (type II) the structural determinants for the targeting to the plasma-membrane lie in the middle part of the protein, in particular in the large cytoplasmic loop, whereas the cytoplasmic N- and C-terminal domains are devoid of such sequences (Lefebvre et al., 2004). Interestingly, replacement of the N- and C-terminal domains of the type II protein Ph AHA2 with those from PH5 are sufficient to convert Ph AHA2 from a plasma membrane into a tonoplast protein, and deletion or replacement of 8 amino acids in the N-terminus of At AHA10 is sufficient to abolishes the tonoplast localization and to direct at least part of the protein to the plasma membrane. This indicates that At AHA10 still contains the (ancestral) determinants for sorting to the plasma membrane and that type III proteins acquired their tonoplast localization via the gain of a vacuolar sorting sequences. It is likely, though not demonstrated, that type III proteins also move via the ER and Golgi, similar to type II proteins, and that the sorting of type II and III proteins deviates at some point, for example the Golgi, because of which they end up in the plasma membrane or tonoplast respectively.

Presumably, the shift from plasma membrane to a tonoplast localization happened early during the evolution of type III proteins, because PH5 homologs from distantly related eudicots, belonging to asterids (petunia), rosids (Arabidopsis, rose, grape) and *Caryophyllales* (carnation), are all targeted to the tonoplast and can substitute PH5. The PH5 homologs from monocots and possibly even gymnosperms are likely to be tonoplast proteins too, because the sequence motif in the N-terminal

domain that is required of tonoplast localization is at least partially conserved in these proteins.

Several observation indicate that type II and III P_{3A}-ATPases also diverged with regard to their post-translational regulation. The YTV motif at the C-terminus of plasma membrane P_{3A}-ATPases is important for pump activity through phosphorylation of the threonine, binding of 14-3-3 proteins to enable formation of an active complex consisting of three P_{3A}-ATPase dimers and six 14-3-3 proteins (Jahn et al., 1997; Fuglsang et al., 1999; Maudoux et al., 2000; Kanczewska et al., 2005; Ottmann et al., 2007). However, the PH5 homologs of angiosperms have a distinct C-terminal motif (HTV or QTV) and the C-terminal domain of PH5 fails to interact with 14-3-3 proteins in yeast. We consider it unlikely that the latter is a false negative result, because this PH5 domain can interact with an AAA-ATPase identified in a yeast two-hybrid screen. In addition, the full PH5 protein is biologically active when expressed in yeast, can form homodimers and bind to PH1, like it does in petunia cells (Verweij et al., 2008; Faraco et al., 2014). Interestingly, the *Picea* PH5 homolog still retained the penultimate tyrosine (Figure 3B), suggesting that this gymnosperm protein may be a transition stage in the divergence of PH5 homologs from other P_{3A}-ATPases. Furthermore, the P_{3B}-ATPase PH1 can bind to PH5 and upregulate its activity (Faraco et al., 2014). Although it is unknown whether the structure of plasma membrane P_{3A}-ATPases would allow binding to PH1, this will in vivo not happen because PH1 is absent from the plasma membrane (Faraco et al., 2014). Similarly, the BRASSINOSTEROID INSENSITIVE (BRI1) receptor can bind and activate only the plasma membrane proteins At AHA1, but not vacuolar P_{3A}-ATPases, as BRI1 resides exclusively in the plasma membrane (Speth et al., 2010).

Although P_{3B}-ATPases were long thought to be unique for prokaryotes, we now found them in all major groups of angiosperms, in a gymnosperm, an alga, several slime molds and several (groups of) fungi. Most if not all of these species contain a single P_{3B}-ATPase gene, except for polyploid angiosperms such as for example *M. domestica* and *Mahinot esculenta*. The phylogenetic and syntenic relationships indicate that the angiosperm homologs apparently evolved by vertical transmission from a common ancestor, which already existed in the earliest angiosperms and apparently even in (some) gymnosperms. The origin of the ancestral spermatophytic gene is, however, less clear.

Several findings suggest that the P_{3B}-ATPases of spermatophytes, fungi and slime molds did not originate by vertical transmission from a single founder gene in a common ancestor, but probably involved one or more horizontal gene transfer (HGT) events. First, the P_{3B}-ATPase from the glomeromycete *Rhizofagus irregularis* does not cluster with P_{3B}-ATPase from other fungal phyla (Supplemental Figures 3 and 4 online). Second, the sequence of the only algal P_{3B}-ATPase that we found (*Chlorella variabilis*) does cluster poorly with the spermatophyte proteins and the encoding genes have entirely different intron exon-architectures, suggesting different origins Third, there are many species (groups) among plants, fungi bacteria and Archaea that lack P_{3B}-ATPases. Although P_{3B}-ATPases were lost several times independently in angiosperms, it seems unlikely that their absence in the 6 primitive plants analyzed (4 unrelated algae, a bryophyte and a lycophyte) and in numerous fungal species is due to multiple independent gene losses in each of these lineages.

Why did plants during evolution recruit the PH1/PH5 pump to acidify vacuoles if they already possessed a V-ATPase? One reason may be that P-ATPases can on thermodynamic grounds generate steeper trans-membrane proton gradients, than V-ATPase, because they hydrolyze more ATP per proton translocated (Rea and Sanders, 1987). Indeed, forced expression of PH1 and PH5 reduced the vacuolar pH in leaf cells of petunia, and, at the same time, strongly down-regulated V-ATPase activity (Faraco et al., 2014). Although the mechanism by which the activity of the PH1/ PH5 pump affects that of the V-ATPase is not clear, this definitely demonstrates that the combination of the two P-ATPases can build larger proton gradient. Hence, the PH1/PH5 pump may have appeared during evolution, in addition to the ubiquitous V-ATPase, to enhance the vacuolar acidification in certain cells for specific new functions.

In petunia the expression of *PH1* and *PH5* confers a reddish color to the flower, which is thought to be important for the attraction of pollinators. This function seems conserved in a distantly related dicot species, because rose petals also express Rh *PH1* and Rh *PH5* and because mutation of the soybean *PH4* homolog also results in a blue flower color (Takahashi et al., 2012), although it remains to be shown that this mutation down regulates the expression of the soybean *PH1* and *PH5* homologs, as in petunia *ph4* mutants. However, this role of PH1 and PH5 in flower pigmentation is unlikely to be their original function, because PH1 and PH5 appeared in plants before flowers (and anthocyanins) evolved.

PH5 in petunia and *At AHA10* in Arabidopsis are needed for the accumulation of tannins in the testa (Baxter et al., 2005; Verweij et al., 2008), presumably because they need to provide the proton gradient that drives the vacuolar sequestration of tannins, or their precursors, via the MATE H^+-antiporter TRANSPARENT TESTA12 (TT12) (Marinova et al., 2007). This role of PH5 is relatively old, as tannins already appeared in ferns (Rausher, 2007), while more primitive plants like *Physcomitrella* and *Selaginella*, which lack PH5, also lack proanthocyanidins (Wolf et al., 2010; Weng and Noel, 2013). The observation that *Nicotiana* expresses its PH5 homolog *PMA9* in a range of (specialized) cell types that lack anthocyanins or tannins, including conductive tissues and various meristems, indicates that PH5-mediated vacuolar acidification may be involved in other processes (Oufattole et al., 2000).

The major function of the P_{3B}-ATPase PH1 seems to be to boost the activity of PH5 in petals, as PH1 has no known activity on its own (Faraco et al., 2014). Although PH1 is in petunia co-expressed with PH5 during seed development, PH5 alone is sufficient for tannin accumulation in *Petunia* and Arabidopsis, which lacks PH1 (Faraco et al., 2014). This may explain why several angiosperms lost PH1 but maintained PH5, whereas the reverse, loss of PH5 alone, was not observed (Figure 9). The P_{3B}-ATPases of fungi, slime molds and prokaryotes, by contrast, must be independent of PH5 homologs, though fungi posses P_{3A}-ATPases. The bacterial proteins can mediate the uptake of Mg^{2+}. However, because this function is redundant with other Mg transporters and the Mg-transport is downhill the electrochemical gradient, which is unusual for an ATP-driven pump, it is doubtful that Mg transport is the primary function of the bacterial proteins (Kehres and Maguire, 2002).

MATERIALS AND METHODS

Identification of P-ATPase genes.

Sequences of PH1 and PH5 homologs from different species were obtained by the screening of the following databases with the petunia protein and nucleotide sequences: Phytozome 9.1: (http://www.phytozome.net/), GenBank (http://www.ncbi.nlm.nih.gov/pubmed), and websites for the genomes of date palm (http://qatar-weill.cornell.edu/research/datepalmGenome/ and PdactyKAsm30_r20101206.fasta.gz to retrieve the scaffolds), *Picea abies* (http://congenie.org/blastsearch/), *Beta vulgaris* (http://bvseq.molgen.mpg.de/blast/),

Vitis vinifera (http://www.genoscope.cns.fr/externe/GenomeBrowser/Vitis/), and *Amborella trichopoda* (www.amborella.org).

Phylogeny analysis

Sequence alignments were generated with MUSCLE and phylogenetic trees were constructed with Maximum likelihood (PhyML) after curation of the alignments by the G-blocks tool, and then rendered by TreeDyn using the online tools at www.Phylogeny.fr and http://phylogeny.lirmm.fr (Dereeper et al., 2008).

Synteny was studied using the Phytozome tool and for *Petunia* we used a 200-kb scaffold containing the *Ph PH1* gene in the middle (Petunia Platform, accession to the petunia genome in preparation).

Genetic stocks

P. hybrida F1 plants (V69 X R159, two *ph5* lines where) used for the expression of the *PH5* homologs, while F2 plants bearing blue-violet flowers from the cross V23 (*ph1*) X V30 (*PH1*) were transformed with constructs for the expression of *PH1* homologs. Grape (*Vitis vinifera* L.) cv. Chardonnay, Barbera, and Pinot plants from a vineyard at Agliano (Piedmont, Italy) were used for gene expression analysis. RNA was extracted as previously reported (Carra et al., 2007). Rose tissues were purchased at the local market.

Quantitative PCR analysis of gene expression

Quantitative RT-PCR was done as described (Faraco et al., 2014), using primers shown in Supplemental Table 4 online.

pH measurement of petunia corolla homogenates

Measures of crude petal extract pH were performed as previously described (Quattrocchio et al., 2006). Measures were repeated for at least five flowers per plant**.**

Constructs for expression of *PH5* and *PH1* homologs

The coding sequence from ATG to STOP (including all introns) of *PH1* and *PH5* homologs from Arabidopsis, carnation (cv.'Moonshadow') and rose (from the local flower market) were amplified from genomic DNA by PCR and cloned between the *p35S promoter* and *p35S terminator* of Cauliflower Mosaic Virus as described

previously for the *p35S:PH5* and *p35S:PH1* constructs (Verweij et al., 2008; Faraco et al., 2014). Because the genomic fragment containing the *Vv PH5* coding sequence (15 Kb) was too long, we tailored (spliced) exons 1 to 9 from the cDNA to a genomic fragment containing exons 10, 11 and 12, and the four contiguous introns, using primers shown in Supplemental Table 3 online.. For the expression of *Vv PH1* we used a chimeric fragment consisting of the spliced exons 1 to 4 from cDNA, the central part (exons 5, 6 and 7, and the intervening introns) from genomic DNA and exon 8 from cDNA using primers shown in Supplemental Table 3 online. As full size At *AHA2* and Ph *AHA2* cDNA were not toxic for *E. coli*, we could use the contiguous coding sequence to generate *p35S:At AHA2* and *p35S:PhAHA2*. All constructs were prepared in the Gateway vectors (destination vector pK2GW7.0) (Karimi et al., 2002). We prepared similar constructs for the expression of the PH5 homologs as GFP fusions. The list of all primers used for the building of the expression clones is given in Supplemental Table 7 online. Immunoblot analysis of total petal protein was performed as previously described (Verweij et al., 2008).

The PhAHA2 coding sequence was amplified from petunia R27 petal cDNA with primers 6341(+attB1) and 6342(+attB2) and used to create a Gateway Entry clone by BP reaction with pDONR P1-P2 (Gateway system, LifeTech) and then recombined into pK7FWG2,0 (Karimi et al., 2002) to obtain *p35S:PhAHA2-GFP*.

For the ^{N}PH5-PhAHA2-^{C}PH5 fusion three different fragments were amplified by PCR: (i) ^{N}PH5 (amino acids 1-29) with primers 4699(+attB1) and 6348, (ii) PhAHA2 (amino acids 25-880) with primers 6347 and 6350 and (iii) ^{C}PH5 (amino acids 885-950) with primers 6349 and 5220(+attB2). The PCR products were purified from gel, mixed in equal molar ratio and used as template for a final PCR amplification with primers 4699(+attB1) and 5220(+attB2). The full-size fragment was inserted in pDONR P1-P2 and subsequently moved to pK7FWG2,0 by Gateway recombination (Life Technologies). All primers sequences are reported in Supplemental Table 7 online.

Constructs for the expression of mutated *p35S:AHA10-GFP* fusions were generated starting from the *p35S:AHA10-GFP* clone by conventional restriction/ligation cloning. Fragments containing the respective mutations were amplified in a series of overlap extension PCRs, using primers shown in Supplemental Table 6 online, and inserted into *Spe*I and PmlI sites of the *AHA10* sequence in the *p35S:AHA10-GFP* plasmid.

Transformation of petunia petal protoplasts and visualization of GFP-fusion proteins con-focal laser scanning microscopy were done as reported previously reported (Faraco et al., 2011).

Tobacco BY2 protoplasts were isolated and transformed as described previously (Appelhagen et al., 2010). Fluorescence was analyzed after 24h incubation in the dark. Bright field and epifluorescence images were obtained with a Leica DM5500 microscope equipped with automated DIC condenser and a fluorescein filterset (Leica filter cube I3). Pictures were taken with Diskus digital imaging software (Technisches Buero Hilgers, Koenigswinter, Germany).

Yeast two hybrid assay

The C-terminal regions of Ph PH5, At AHA2 and Ph AHA2 were amplified by PCR using primers shown in Supplemental Table 6 online and cloned into pENTR/D and pDONR207 from Invitrogen by a BP reaction (Life Technologies). The Entry clones were then used to recombine the fragments into Gateway Y2H vectors for the expression of fusions to the AD or BD domain of GAL4 (Stratagene vectors pAD-GAL4 and pBD-GAL4 Cam in which we have cloned a attR1-attR2 cassette to make them Gateway compatible). The Ph PH5 C-terminal domain chosen consists of the last 100 amino-acids of the protein (amino-acid 838 to stop), that of PhAHA2 of 106 amino acids (AA 847 to stop) and that of AtAHA2 of 105 amino acids of the Ph PH5 protein (AA 844 to stop). The Ph *14-3-3 chi, kappa, omega, omicron* and *psi* coding sequences in the pAD-GAL4 vector were obtained by screening a cDNA library with pBEH2 in pBD-GAL4 (Verhoef et al., 2013).

Ph *AAA-ATPase* coding sequence in the pAD-GAL4 vector was obtained by screening a cDNA library of petunia line R27 petals with the *Ph PH5* C-terminal region in pBD-GAL4.

SUPPLEMENTAL DATA

The following materials are available:

- **Supplemental Figure 1**. Expression of transgenes in ph5 and ph1 mutants transformed respectively with constructs for the expression of PH5 homologs, PH1 homologues and AtAHA2 in petals of transgenic plants.

- **Supplemental Figure 2.** Alignment of PH1 homologues from petunia (Ph), grape (Vv) and rose (Rh).
- **Supplemental Figure 3.** Phylogenetic tree shows clustering of partial *Picea abies* and *Persea americana* P_{3B}-ATPase sequences with Angiosperm homologs**.**
- **Supplemental Figure 4**. Phylogenetic tree of PH1 homologs from a large selection of plants, protozoan, algae, bacteria and archaea.
- **Supplemental Figure 5.** Identifty of the genes appearing in the synteny analysis of the PH1 locus in different species presented in Figure 10.
- **Supplemental Figure 6.** Alignment, in Clustal format, of P_{3A}-ATPases used to produce the phylogenetic tree in Figure 2.
- **Supplemental Figure 7**. Alignment, in Clustal format, of P_{3B}-ATPases used to produce the phylogenetic tree in Figure 8.
- **Supplemental Figure 8.** Curated alignment (Clustal format) used to produce the phylogenetic tree in Supplemental Figure 3.
- **Supplemental Figure 9.** Curated sequence alignment (Clustal format) used to produce the phylogenetic tree in Supplemental Figure 4

ACCESSION NUMBERS

P. inflata AHA2 XXXXXX; *P. dactylifera* P_{3A}-ATPase XXXX, *P. dactylifera* PH5 homolog XXXX, *R. hybrida* PH5 homolog XXXXX, *D. caryophyllus* PH5 homolog XXXXX, *P. abies* PH5 homologue XXXXXX, *P. dactylifera* PH1 homolog XXXX, *R. hybrida* PH1 homolog XXXX,

ACKNOWLEDGMENTS

We are grateful to Drs. Yoshikazu Tanaka and Masako Fukuchi-Mizutani (Suntory Global Innovation Center, Osaka Japan) for providing the sequence of the rose PH5 homolog, to the Petunia community for access to the (unpublished) petunia genome sequence, and to Erik Manders and Ronald Breedijk (Center of Advanced Microscopy, University of Amsterdam) for help with con-focal microscopy.

AUTHOR CONTRIBUTIONS:

S.P., M.B., C.S., Y.L., I.A., L.M.de F. and W.V. performed the experiments; S.P., M.B., C.S., Y.L., A.S., M.S., B.W., R.K. and F.Q. analyzed data; S.P., B.W., M.S, R.K. and F.Q. wrote the paper.

FIGURE LEGENDS

Figure 1. Similarity of sequences and gene architecture among different P_{3A}ATPases.
(A) Alignment of the protein sequences of PH5 homologs from carnation (Dc PH5), *Brachypodium* (Bd PH5), rice (OsAHA9), grape (Vv PH5) and rose (Rh PH5) and the type I Arabidopsis plasma membrane protein At AHA4.
(B) Diagram depicting the gene architecture of several members of the P_{3A} family. Arrows indicate exons.

Figure 2. Phylogenetic analysis of selected P_{3A}-ATPases showing that PH5 homologs are wide spread among angiosperms. For each species the proteins with most similarity to At AHA2 (type II) and to Ph PH5 are shown. In addition we added the type I protein At AHA4. Note that for some species the protein with most similarity to PH5 belongs to a different P_{3A}-ATPAse clade indicating that a true PH5 ortholog is missing in that species. The alignment used to build this phylogenetic tree is shown in Supplemental Figure 6 online.

Figure 3. PH5 homologs are functionally conserved.
(***A***) Complementation of a petunia *PH5* mutant phenotype with PH5 homologs from different species. The bar next to each flower represents the average pH of the crude petal extract ($n \geq 5$, ±SD). Note that all proteins, except AtAHA2, correct the *ph* phenotype.
(**B**) Confocal images of the subcellular localization of AHA2 and PH5 homologs. RFP-AtSYP122 marks the plasma membrane. AtAHA2-GFP and PhAHA2GFP colocalize with RFP-AtSYP122, while the PH5 homologs result in green fluorescence on the tonoplast (as better visible in the inserts). The size bar is 10µm.
(**C**) Immunoblot of proteins from plants expressing Ph PH5-GFP or Rh PH5-GFP probed with anti-GFP.

Figure 4. Comparison of the N- and C-terminal sequences of different P_{3A}-ATPases.
(A) Alignment of the N-terminal domain of several P_{3A}-ATPases.
(B) Alignment of the C-terminal portion of several plant P_{3A}-ATPases. The red asterisk marks the conserved tyrosine residue (Y) that is phosphorylated in AtAHA2

homologs to enable interaction with 14-3-3 proteins. A list of the species is available in The Supplemental Table 1 online.

Figure 5. The terminal domains of PH5 direct tonoplast localization.
(A) Diagram of the constructs for the expression of GFP fusion proteins used in the experiment in B. The numbers indicate the amino acids within the proteins.
(B) Confocal images of BY2 protoplasts expressing PhAHA2-GFP, which co-localizes with RFP-At SYP122 (red signal) in the plasma membrane and of the ^{N}PH5-PhAHA2-^{C}PH5-GFP, which marks th tonoplast

Figure 6. The N-terminal domain is required for tonoplast localization of At AHA10.
(A) Mutations built in the N-termini in the AHA10 proteins expressed in B.
(B) Fluorescence microscopy and brightfield images of the localization of AHA10 mutants in tobacco BY2 protoplasts. AHA2-GFP localizes on the plasma membrane that appears as a perfect circle. PH5-GFP and the wild type AHA10-GFP fusions localize on the tonoplast marking the numerous invagination of the vacuolar membrane. All three AHA10 mutants fail in localizing at the tonoplast and give instead signal on the plasma membrane associated with diffused fluorescence. The size bar is 10μm

Figure 7. Yeast 2-hybrid analysis of the interactions of P_{3A}-ATPases with 14-3-3 proteins. Interactions are seen as growth on plates lacking histidine and expression of lacZ reporter activity (blue stain). The petunia AAA-ATPase protein is used as positive control for the C-terminal region of PH5. PhBEH2, a member of the BES1/BZR1 family of transcription factors was shown previously to interact with all the 14-3-3 proteins used in this assay (Verhoef et al., 2013).

Figure 8. PH1 homologs in bacterial and plant species.
(**A**) Phenotype of *PH1* mutant petunia flowers complemented with transgenes expressing PH1 homologs from different species. The bar next to the flowers represents the average pH of the crude petal extract (N≥5, ±SD).

(**B**) Phylogenetic tree of proteins from distinct species with highest similarity to PH1. The alignement used to build this phylogenetic tree is shown in Supplemental Figure 2 online

Figure 9. Distribution of PH1 and PH5 homologs in the plant kingdom Green checks (√) indicates the presence of a homolog, a red cross (X) its absence and ? indicates uncertainty because no completely sequenced genome is available

Figure 10. Synteny analysis of the genomic regions containing *PH1* homologs.
The arrows denote genes and their orientation lying immediately upstream and downstream the PH1 homologs in different species. Equal numbers and fill color indicate similarity of genes from *Phaseolus vulgaris* (Pv), *Gossypium raimondii* (Gr), *Teobroma cacao* (Tc), *Manihot esculenta* (Me), *Ricinus communis* (Rc), *Carica papaya* (Cp), *Petunia hybrida* (Ph), *Fragaria vesca* (Fv), *Vitis vinifera* (Vv), *Eucalyptus grandis* (Eg) and syntenic regions from *Arabidopsis thaliana* (At), *Capsella rubella* (Cr), *Solanum lycopersicum* (Sl), *Solanum tuberosum* (St), which lack a PH1 homologous genes. The maps are not drawn to scale; details on encoded proteins are given in Supplemental Figure 4 online. In Arabidopsis (At) a genomic fragment containing some genes belonging to this region is found elsewhere in the genome. In potato (St), of the gene flanking immediately *PH1* on the right side (7= Glucan 1,3-beta-glucosidase) only a fragment is left, indicating that the breakpoint that lead to the loss of PH1 occurred within the gene sequence.

Figure 11. RT-PCR analysis of the expression of rose and grape homologs of PH1 and PH5.
(**A**) Accumulation of anthocyanin pigments during development of Barbera en Pinot berries. In Barbera veraison (arrow) occurs two weeks later than in the other two varieties.
(**B**) Relative expression of Vv *PH1* and Vv *PH5* in developing chardonay, pinot and barbera berries. The arrow indicates véraison. Expression in berries of Chardonnay 20 days after anthesis has been chosen as reference.
(C) Expression of Rh *PH1* and Rh *PH5* in the last stages of the development of the flower buds and in the leaves of rose.

REFERENCES

Appelhagen, I., Huep, G., Lu, G.H., Strompen, G., Weisshaar, B., and Sagasser, M. (2010). Weird fingers: functional analysis of WIP domain proteins. FEBS Lett **584,** 3116-3122.

Arango, M., Gevaudant, F., Oufattole, M., and Boutry, M. (2003). The plasma membrane proton pump ATPase: the significance of gene subfamilies. Planta **216,** 355-365.

Assaad, F.F., Qiu, J.L., Youngs, H., Ehrhardt, D., Zimmerli, L., Kalde, M., Wanner, G., Peck, S.C., Edwards, H., Ramonell, K., Somerville, C.R., and Thordal-Christensen, H. (2004). The PEN1 syntaxin defines a novel cellular compartment upon fungal attack and is required for the timely assembly of papillae. Molecular biology of the cell **15,** 5118-5129.

Axelsen, K.B., and Palmgren, M.G. (1998). Evolution of substrate specificities in the P-type ATPase superfamily. J Mol Evol **46,** 84-101.

Axelsen, K.B., Venema, K., Jahn, T., Baunsgaard, L., and Palmgren, M.G. (1999). Molecular dissection of the C-terminal regulatory domain of the plant plasma membrane H^+-ATPase AHA2: mapping of residues that when altered give rise to an activated enzyme. Biochemistry-Us **38,** 7227-7234.

Baxter, I., Tchieu, J., Sussman, M.R., Boutry, M., Palmgren, M.G., Gribskov, M., Harper, J.F., and Axelsen, K.B. (2003). Genomic comparison of P-type ATPase ion pumps in Arabidopsis and rice. Plant Physiol **132,** 618-628.

Baxter, I.R., Young, J.C., Armstrong, G., Foster, N., Bogenschutz, N., Cordova, T., Peer, W.A., Hazen, S.P., Murphy, A.S., and Harper, J.F. (2005). A plasma membrane H+-ATPase is required for the formation of proanthocyanidins in the seed coat endothelium of Arabidopsis thaliana. Proc Natl Acad Sci U S A **102,** 2649-2654.

Beyenbach, K.W., and Wieczorek, H. (2006). The V-type H+ ATPase: molecular structure and function, physiological roles and regulation. The Journal of experimental biology **209,** 577-589.

Carra, A., Gambino, G., and Schubert, A. (2007). A cetyltrimethylammonium bromide-based method to extract low-molecular-weight RNA from polysaccharide-rich plant tissues. Anal Biochem **360,** 318-320.

Dereeper, A., Guignon, V., Blanc, G., Audic, S., Buffet , S., Chevenet, F., Dufayard, J.F., Guindon, S., Lefort , V., Lescot, M., Claverie, J.M., and Gascuel, O. (2008). Phylogeny.fr: robust phylogenetic analysis for the non-specialist. Nucleic Acids Res. **1.**

DeWitt, N.D., and Sussman, M.R. (1995). Immunocytological localization of an epitope-tagged plasma membrane proton pump (H(+)-ATPase) in phloem companion cells. Plant Cell **7,** 2053-2067.

DeWitt, N.D., Hong, B., Sussman, M.R., and Harper, J.F. (1996). Targeting of two Arabidopsis H(+)-ATPase isoforms to the plasma membrane. Plant Physiol **112,** 833-844.

Drozdowicz, Y.M., and Rea, P.A. (2001). Vacuolar H(+) pyrophosphatases: from the evolutionary backwaters into the mainstream. Trends in plant science **6,** 206-211.

Duby, G., and Boutry, M. (2009). The plant plasma membrane proton pump ATPase: a highly regulated P-type ATPase with multiple physiological roles. Pflugers Arch **457,** 645-655.

Faraco, M. (2011). PhD thesis. VU University Amsterdam.

Faraco, M., Di Sansebastiano, G.P., Spelt, K., Koes, R., and Quattrocchio, F.M. (2011). One protoplast is not the other. Plant Physiol **156,** 474-478.

Faraco, M., Spelt, C., Bliek, M., Verweij, W., Hoshino, A., Espen, L., Prinsi, B., Jaarsma, R., Tarhan, E., de Boer, A.H., Di Sansebastiano, G.P., Koes, R., and

Quattrocchio, F.M. (2014). Hyperacidification of vacuoles by the combined action of two different P-ATPases in the tonoplast determines flower color. Cell reports **6,** 32-43.

Fuglsang, A.T., Visconti, S., Drumm, K., Jahn, T., Stensballe, A., Mattei, B., Jensen, O.N., Aducci, P., and Palmgren, M.G. (1999). Binding of 14-3-3 protein to the plasma membrane H(+)-ATPase AHA2 involves the three C-terminal residues Tyr(946)-Thr-Val and requires phosphorylation of Thr(947). J Biol Chem **274,** 36774-36780.

Gaxiola, R.A., Palmgren, M.G., and Schumacher, K. (2007). Plant proton pumps. FEBS Lett **581,** 2204-2214.

Iyer, L.M., Leipe, D.D., Koonin, E.V., and Aravind, L. (2004). Evolutionary history and higher order classification of AAA+ ATPases. Journal of structural biology **146,** 11-31.

Jahn, T., Fuglsang, A.T., Olsson, A., Bruntrup, I.M., Collinge, D.B., Volkmann, D., Sommarin, M., Palmgren, M.G., and Larsson, C. (1997). The 14-3-3 protein interacts directly with the C-terminal region of the plant plasma membrane H(+)-ATPase. Plant Cell **9,** 1805-1814.

Kanczewska, J., Marco, S., Vandermeeren, C., Maudoux, O., Rigaud, J.L., and Boutry, M. (2005). Activation of the plant plasma membrane H+-ATPase by phosphorylation and binding of 14-3-3 proteins converts a dimer into a hexamer. Proc Natl Acad Sci U S A **102,** 11675-11680.

Karimi, M., Inze, D., and Depicker, A. (2002). GATEWAY vectors for Agrobacterium-mediated plant transformation. Trends in plant science **7,** 193-195.

Kehres, D.G., and Maguire, M.E. (2002). Structure, properties and regulation of magnesium transport proteins. Biometals **15,** 261-270.

Kim, D.H., Eu, Y.J., Yoo, C.M., Kim, Y.W., Pih, K.T., Jin, J.B., Kim, S.J., Stenmark, H., and Hwang, I. (2001). Trafficking of phosphatidylinositol 3-phosphate from the trans-Golgi network to the lumen of the central vacuole in plant cells. Plant Cell **13,** 287-301.

Kobayashi, S., Goto-Yamamoto, N., and Hirochika, H. (2004). Retrotransposon-induced mutations in grape skin color. Science **304,** 982.

Koes, R., Verweij, C.W., and Quattrocchio, F. (2005). Flavonoids: a colorful model for the regulation and evolution of biochemical pathways. Trends Plant Sci. **5,** 236-242.

Kuhlbrandt, W. (2004). Biology, structure and mechanism of P-type ATPases. Nat Rev Mol Cell Biol **5,** 282-295.

Lefebvre, B., Batoko, H., Duby, G., and Boutry, M. (2004). Targeting of a *Nicotiana plumbaginifolia* H^+-ATPase to the plasma membrane is not by default and requires cytosolic structural determinats. Plant Cell **16,** 1772-1789.

Lefebvre, B., Arango, M., Oufattole, M., Crouzet, J., Purnelle, B., and Boutry, M. (2005). Identification of a Nicotiana plumbaginifolia plasma membrane H(+)-ATPase gene expressed in the pollen tube. Plant Mol Biol **58,** 775-787.

Marinova, K., Pourcel, L., Weder, B., Schwarz, M., Barron, D., Routaboul, J.M., debeaujon, I., and Klein, M. (2007). The Arabidopsis MATE transporter TT12 acts as a vacuolar flavonoid/H^+-antiporter active in proanthocyanidin-accumulating cells of the seed coat. Plant Cell **19,** 2023-2038.

Maudoux, O., Batoko, H., Oecking, C., Gevaert, K., Vandekerckhove, J., Boutry, M., and Morsomme, P. (2000). A plant plasma membrane H+-ATPase expressed in yeast is activated by phosphorylation at its penultimate residue and binding of 14-3-3 regulatory proteins in the absence of fusicoccin. J Biol Chem **275,** 17762-17770.

Muller, M.L., and Taiz, L. (2002). Regulation of the lemon-fruit V-ATPase by variable stoichiometry and organic acids. J Membr Biol **185,** 209-220.

Nelson, N., Perzov, N., Cohen, A., Hagai, K., Padler, V., and Nelson, H. (2000). The cellular biology of proton-motive force generation by V-ATPases. The Journal of experimental biology **203,** 89-95.

Ottmann, C., Marco, S., Jaspert, N., Marcon, C., Schauer, N., Weyand, M., Vandermeeren, C., Duby, G., Boutry, M., Wittinghofer, A., Rigaud, J.L., and Oecking, C. (2007). Structure of a 14-3-3 coordinated hexamer of the plant plasma membrane H^+ -ATPase by combining X-ray crystallography and electron cryomicroscopy. Mol Cell **25,** 427-440.

Oufattole, M., Arango, M., and Boutry, M. (2000). Identification and expression of three new Nicotiana plumbaginifolia genes which encode isoforms of a plasma-membrane H(+)-ATPase, and one of which is induced by mechanical stress. Planta **210,** 715-722.

Palmgren, M.G. (2001). Plant plasma mebrane H^+-ATPases: Powerhouses for nutrient uptake. Annu Rev Plant Physiol Plant Mol Biol **52,** 817-845.

Palmgren, M.G., and Nissen, P. (2011). P-type ATPases. Annu Rev Biophys **40,** 243-266.

Pedersen, B.P., Buch-Pedersen, M.J., Morth, J.P., Palmgren, M.G., and Nissen, P. (2007). Crystal structure of the plasma membrane proton pump. Nature **450,** 1111-1114.

Pedersen, C.N., Axelsen, K.B., Harper, J.F., and Palmgren, M.G. (2012). Evolution of plant p-type ATPases. Front Plant Sci **3,** 31.

Piotrowski, M., Morsomme, P., Boutry, M., and Oecking, C. (1998). Complementation of the Saccharomyces cerevisiae plasma membrane H+-ATPase by a plant H+-ATPase generates a highly abundant fusicoccin binding site. J Biol Chem **273,** 30018-30023.

Quattrocchio, F., Verweij, W., Kroon, A., Spelt, C., Mol, J., and Koes, R. (2006). PH4 of petunia is an R2R3-MYB protein that activates vacuolar acidification through interactions with Basic-Helix-Loop-Helix transcription factors of the anthocyanin pathway. Plant Cell **18,** 1274-1291.

Quattrocchio, F., Wing, J., van der Woude, K., Souer, E., de Vetten, N., Mol, J., and Koes, R. (1999). Molecular analysis of the *anthocyanin2* gene of *Petunia* and its role in the evolution of flower color. Plant Cell **11,** 1433-1444.

Quattrocchio, F.M., Spelt, C., and Koes, R. (2013). Transgenes and protein localization: myths and legends. Trends in plant science **18,** 473-476.

Rausher, M.D. (2007). The evolution of flavonoids and their genes. In The Science of Flavonoids, E. Grotewold, ed (Springer), pp. 175-211.

Rea, P.A., and Sanders, D. (1987). Tonplast energization: Two H+ pumps, one membrane. Physiol Plantarum **71,** 131-141.

Schumacher, K., and Krebs, M. (2010). The V-ATPase: small cargo, large effects. Curr Opin Plant Biol **13,** 724-730.

Smith, R.L., and Maguire, E.M. (1998a). Microbial magnesium transport: unusual transporters searching for identity. Mol Microbiol **28,** 217-226.

Smith, R.L., and Maguire, M.E. (1998b). Microbial magnesium transport: unusual transporters searching for identity. Mol Microbiol **28,** 217-226.

Spelt, C., Quattrocchio, F., Mol, J., and Koes, R. (2002). *ANTHOCYANIN1* of petunia controls pigment synthesis, vacuolar pH, and seed coat development by genetically distinct mechanisms. Plant Cell **14,** 2121-2135.

Speth, C., Jaspert, N., Marcon, C., and Oecking, C. (2010). Regulation of the plant plasma membrane H+-ATPase by its C-terminal domain: what do we know for sure? European journal of cell biology **89,** 145-151.

Svennelid, F., Olsson, A., Piotrowski, M., Rosenquist, M., Ottman, C., Larsson, C., Oecking, C., and Sommarin, M. (1999). Phosphorylation of Thr-948 at the C terminus of the plasma membrane H(+)-ATPase creates a binding site for the regulatory 14-3-3 protein. Plant Cell **11,** 2379-2391.

Taiz, L. (1992). The plant vacuole. J. Exp. Biol. **172,** 113-122.

Takahashi, R., Yamagishi, N., and Yoshikawa, N. (2012). A MYB transcription factor controls flower color in soybean. J Hered.

Ulaszewski, S., Grenson, M., and Goffeau, A. (1983). Modified plasma-membrane ATPase in mutants of Saccharomyces cerevisiae. European journal of biochemistry / FEBS **130,** 235-239.

Verhoef, N., Yokota, T., Shibata, K., de Boer, G.J., Gerats, T., Vandenbussche, M., Koes, R., and Souer, E. (2013). Brassinosteroid biosynthesis and signalling in Petunia hybrida. J Exp Bot **64,** 2435-2448.

Verweij, W., Spelt, C., Di Sansebastiano, G.P., Vermeer, J., Reale, L., Ferranti, F., Koes, R., and Quattrocchio, F. (2008). An H^+ P-ATPase on the tonoplast determines vacuolar pH and flower colour. Nature cell biology **10,** 1456-1462.

Weng, J.K., and Noel, J.P. (2013). Chemodiversity in Selaginella: a reference system for parallel and convergent metabolic evolution in terrestrial plants. Front Plant Sci **4,** 119.

Wolf, L., Rizzini, L., Stracke, R., Ulm, R., and Rensing, S.A. (2010). The molecular and physiological responses of Physcomitrella patens to ultraviolet-B radiation. Plant Physiol **153,** 1123-1134.

Yazaki, Y. (1976). Co-pigmentation and the color change with age in petals of Fuchsia hybrida. Journal of plant research **89,** 45-57.

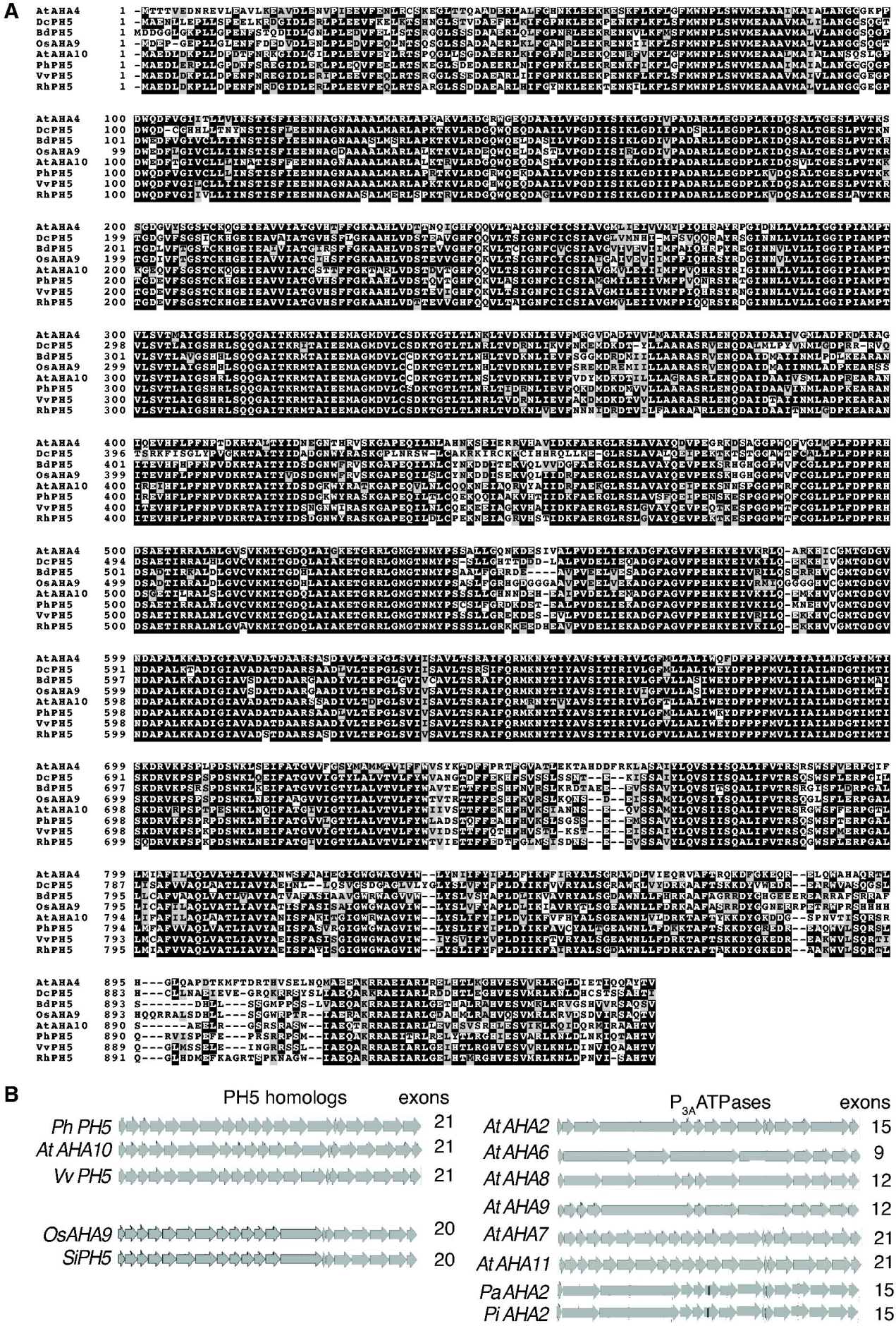

Figure 1. Similarity of sequences and gene architecture among different P_{3A}-ATPases.
(**A**) Alignment of the protein sequences of PH5 homologs from carnation (Dc PH5), Brachypodium (Bd PH5), rice (OsAHA9), grape (Vv PH5) and rose (Rh PH5) and the type I Arabidopsis plasma membrane protein At AHA4.
(**B**) Diagram depicting the gene architecture of several members of the P3A family. Arrows indicate exons.

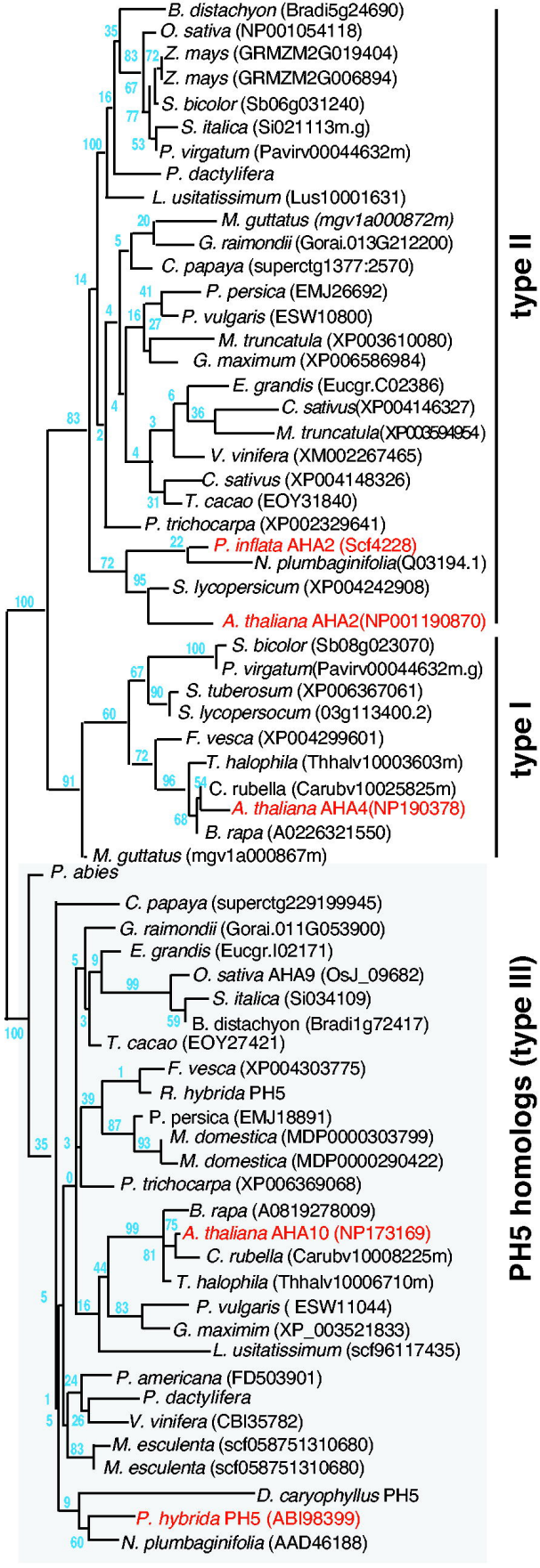

Figure 2. Phylogenetic analysis of selected P3A-ATPases showing that PH5 homologs are wide spread among Angiosperms. For each species the proteins with most similarity to At AHA2 (type II) and to Ph PH5 are shown. In addition we added the type I protein At AHA4. Note that for some species the protein with most similarity to PH5 belongs to a different P3A-ATPAse clade indicating that a true PH5 ortholog is missing in that species. The alignment used to build this phylognetic tree is shown in Supplemental Figure 6 online. The blue numbers indicate boots trap support (% of 500 replicas).

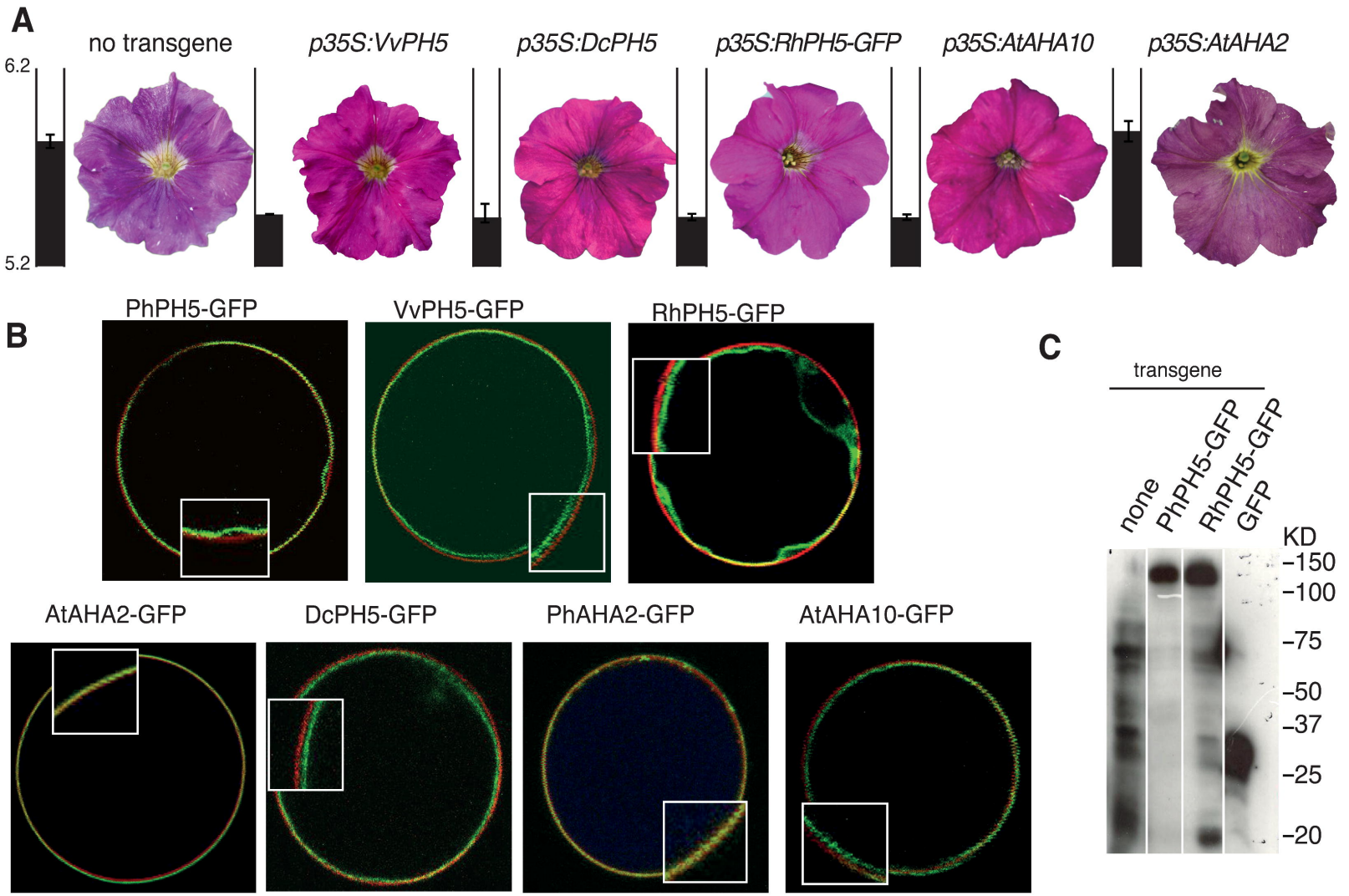

Figure 3. PH5 homologs are functionally conserved.

(**A**) Complementation of a petunia PH5 mutant phenotype with PH5 homologs from different species. The bar next to each flower represents the average pH of the crude petal extract (n≥5, ±SD). Note that all proteins, except AtAHA2, correct the ph phenotype.

(**B**) Confocal images of the subcellular localization of AHA2 and PH5 homologs. RFP-AtSYP122 marks the plasma membrane. AtAHA2-GFP and PhAHA2GFP colocalize with RFP-AtSYP122, while the PH5 homologs result in green fluorescence on the tonoplast (as better visible in the inserts). The size bar is 10μm.

(**C**) Immunoblot of proteins from plants expressing Ph PH5-GFP or Rh PH5-GFP probed with anti-GFP.

Figure 4. Comparison of the N- and C-terminal sequences of different P3A-ATPases.
(**A**) Alignment of the N-terminal domain of several P3A-ATPases.
(**B**) Alignmemnt of the C-terminal portion of several plant P3A-ATPases. The red asterisk marks the conserved tyrosine residue (Y) that is phosphorylated in AtAHA2 homologs to enable interaction with 14-3-3 proteins. A list of the species is available in the Supplemental Table 1 online.

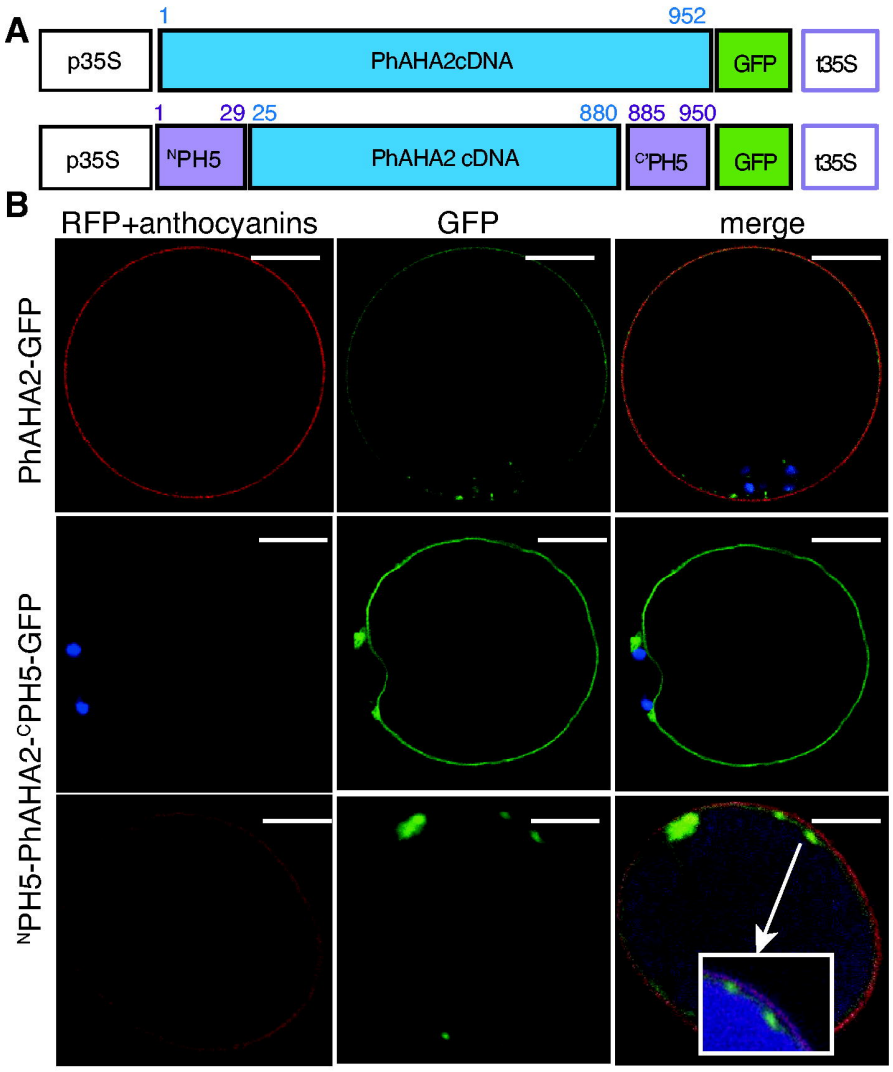

Figure 5. The terminal domains of PH5 direct tonoplast localization.

(**A**) Diagram of the constructs for the expression of GFP fusion proteins used in the experiment in B. The numbers indicate the amino acids within the proteins.

(**B**) Confocal images of BY2 protoplasts expressing Ph AHA2-GFP, which co-localizes with RFP-At SYP122 (red signal) in the plasma membrane and of the NPH5-PhAHA2-CPH5-GFP, which marks the tonoplast.

The size bar is 10µm

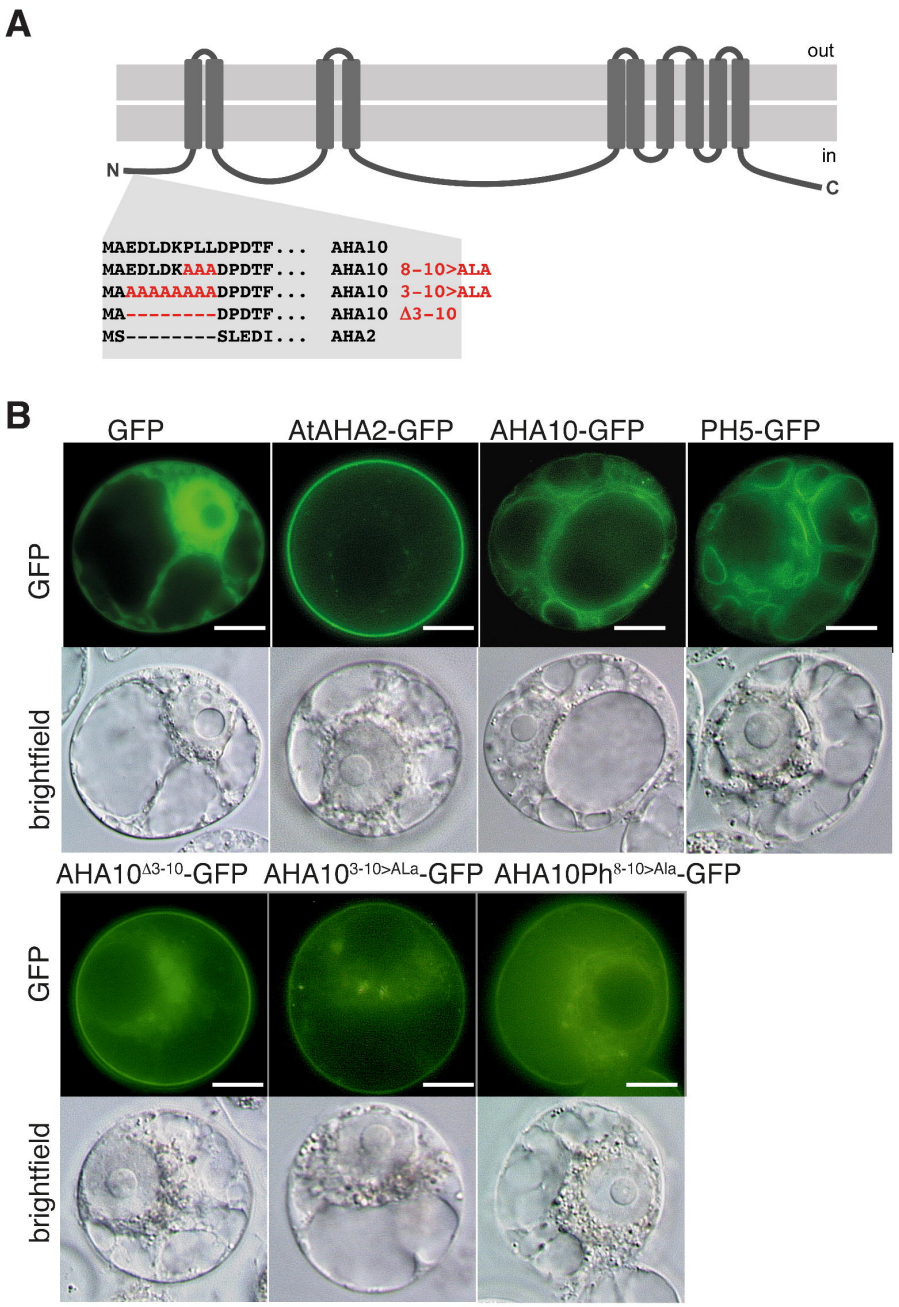

Figure 6. The N-terminal domain is required for tonoplast localization of At AHA10. (**A**) Mutations built in the N-termini in the AHA10 proteins expressed in B. (**B**) Fluorescence microscopy and brightfield images of the localization of AHA10 mutants in tobacco BY2 protoplasts. AHA2-GFP localizes on the plasma membrane that appears as a perfect circle. PH5-GFP and the wild type AHA10-GFP fusions localize on the tonoplast marking the numerous invagination of the vacuolar membrane. All three AHA10 mutants fail in localizing at the tonoplast and give instead signal on the plasma membrane associated with diffused fluorescence .
The size bar is 10µm.

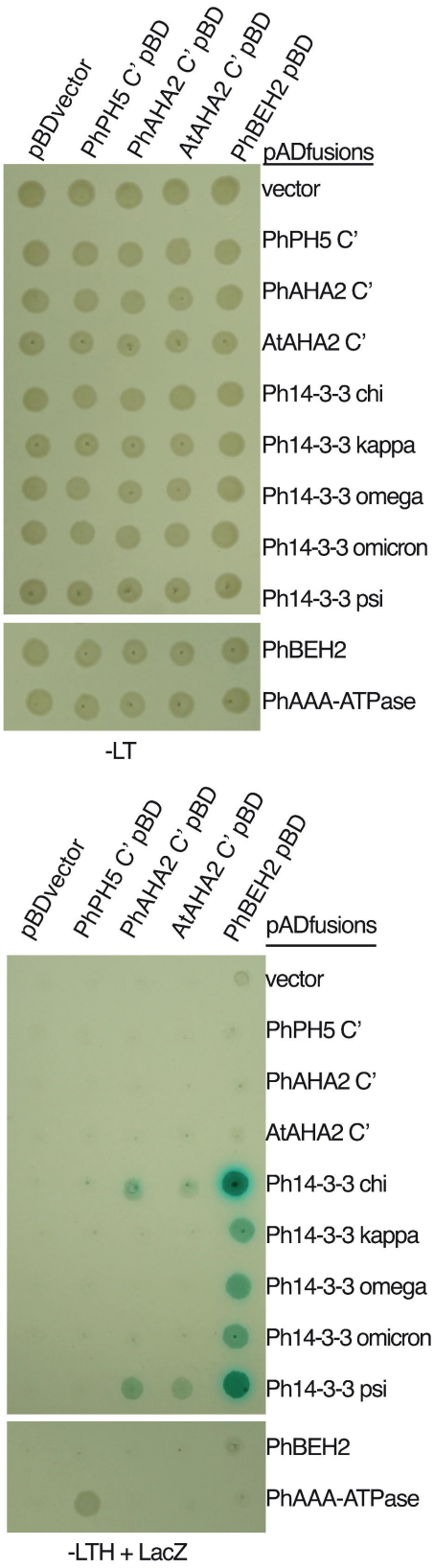

Figure 7. Yeast 2-hybrid analysis of the interactions of P3A-ATPases with 14-3-3 proteins. Interactions are seen as growth on plates lacking histidine and expression of lacZ reporter activity (blue stain). The petunia AAA-ATPase protein is used as positive control for the C-terminal region of PH5. PhBEH2, a member of the BES1/BZR1 family of transcription factors was shown previously to interact with all the 14-3-3 proteins used in this assay (Verhoef et al., 2013).

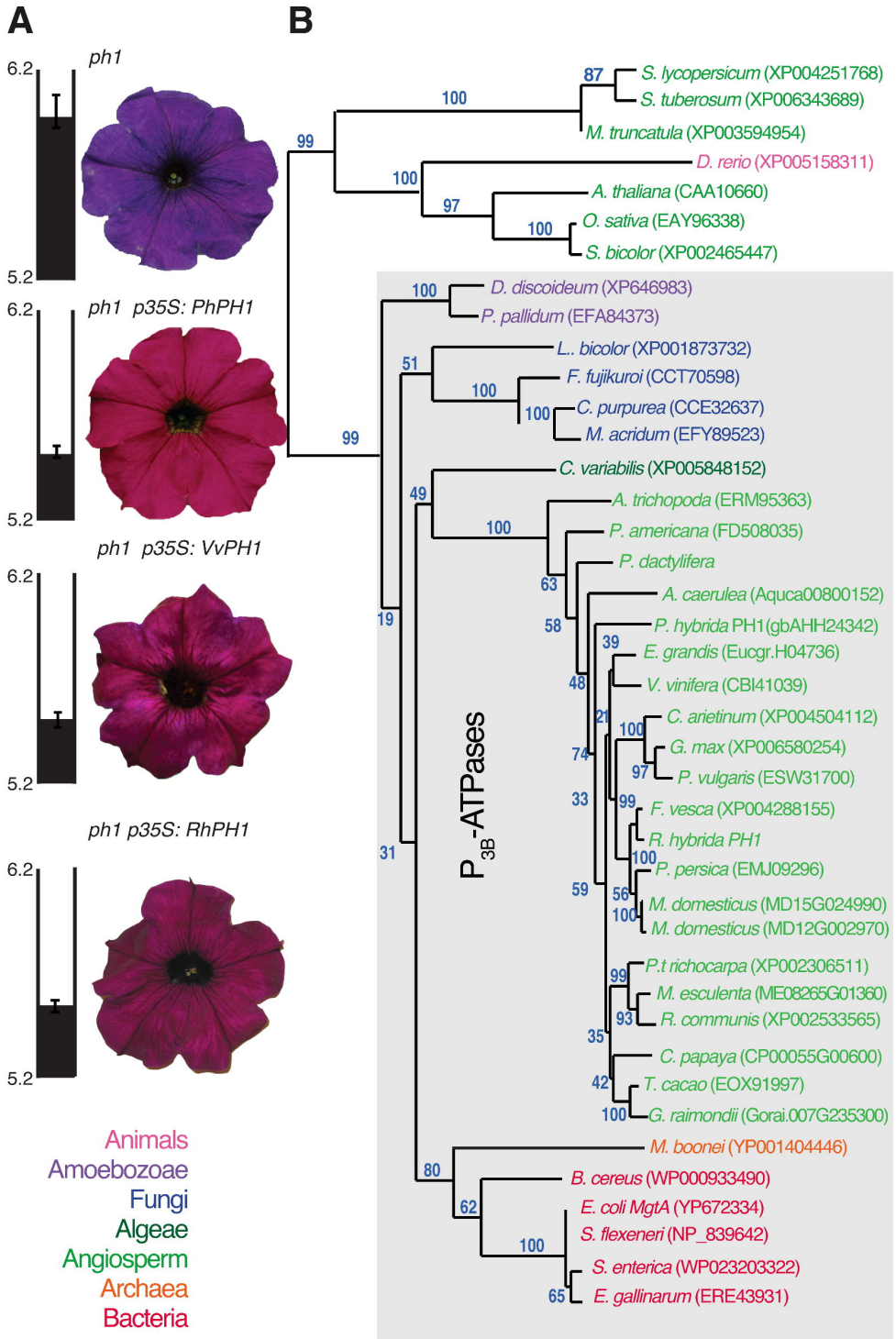

Figure 8. PH1 homologs in bacteriall and plant species.

(**A**) Phenotype of PH1 mutant petunia flowers complemented with transgenes expressing PH1 homologs from different species. The bar next to the flowers represents the average pH of the crude petal extract (N≥5, ±SD).

(**B**) Phylogenetic tree of proteins from distinct species with highest similarity to PH1. The alignement used to build this phylogenetic tree is shown in Supplemental Figure 2 online. The blue numbers indicate boots trap support (% of 500 replicas).

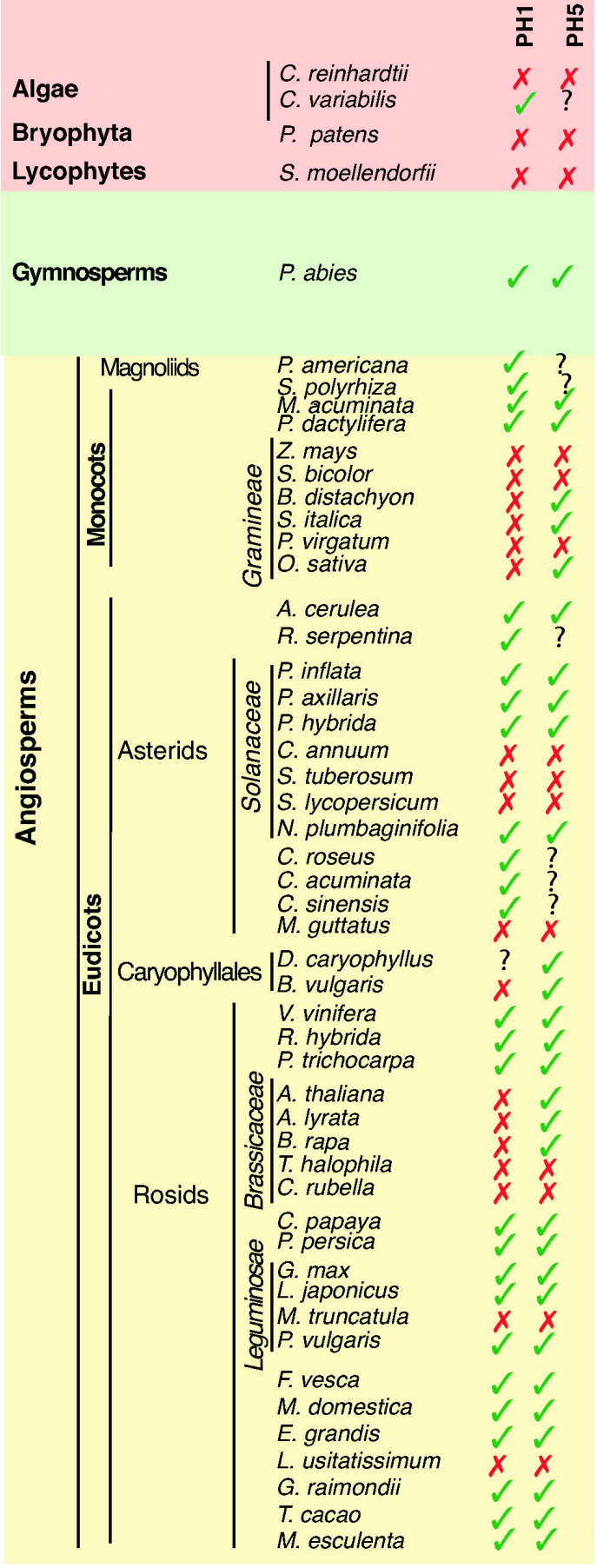

Figure 9. Distribution of PH1 and PH5 homologs in the plant kingdom Green checks (√) indicates the presence of a homolog, a red cross (X) its absence and ? indicates uncertainty because no completely sequenced genome is available

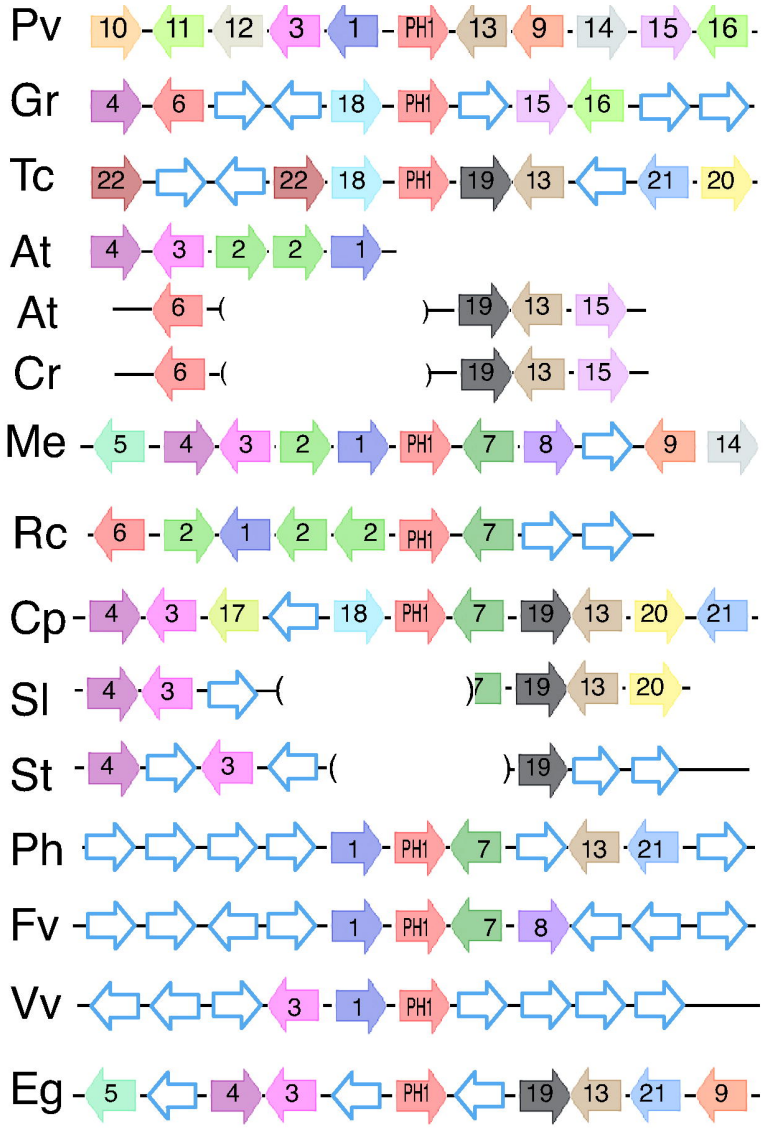

Figure 10. Synteny analysis of the genomic regions containing PH1 homologs.
The arrows denote genes and their orientation lying immediately upstream and downstream the PH1 homologs in different species. Equal numbers and fill color indicate similarity of genes from Phaseolus vulgaris (Pv), Gossypium raimondii (Gr), Teobroma cacao (Tc), Manihot esculenta (Me), Ricinus communis (Rc), Carica papaya (Cp), Petunia hybrida (Ph), Fragaria vesca (Fv), Vitis vinifera (Vv), Eucalyptus grandis (Eg) and syntenic regions from Arabidopsis thaliana (At), Capsella rubella (Cr), Solanum lycopersicum (Sl), Solanum tuberosum (St), which lack a PH1 homologous genes. The maps are not drawn to scale; details on encoded proteins are given in Supplemental Figure 4 online. In Arabidopsis (At) a genomic fragment containing some genes belonging to this region is found elsewhere in the genome. In potato (St), of the gene flanking immediately PH1 on the right side (7= Glucan 1,3-beta-glucosidase) only a fragment is left, indicating that the breakpoint that lead to the loss of PH1 occurred within the gene sequence.

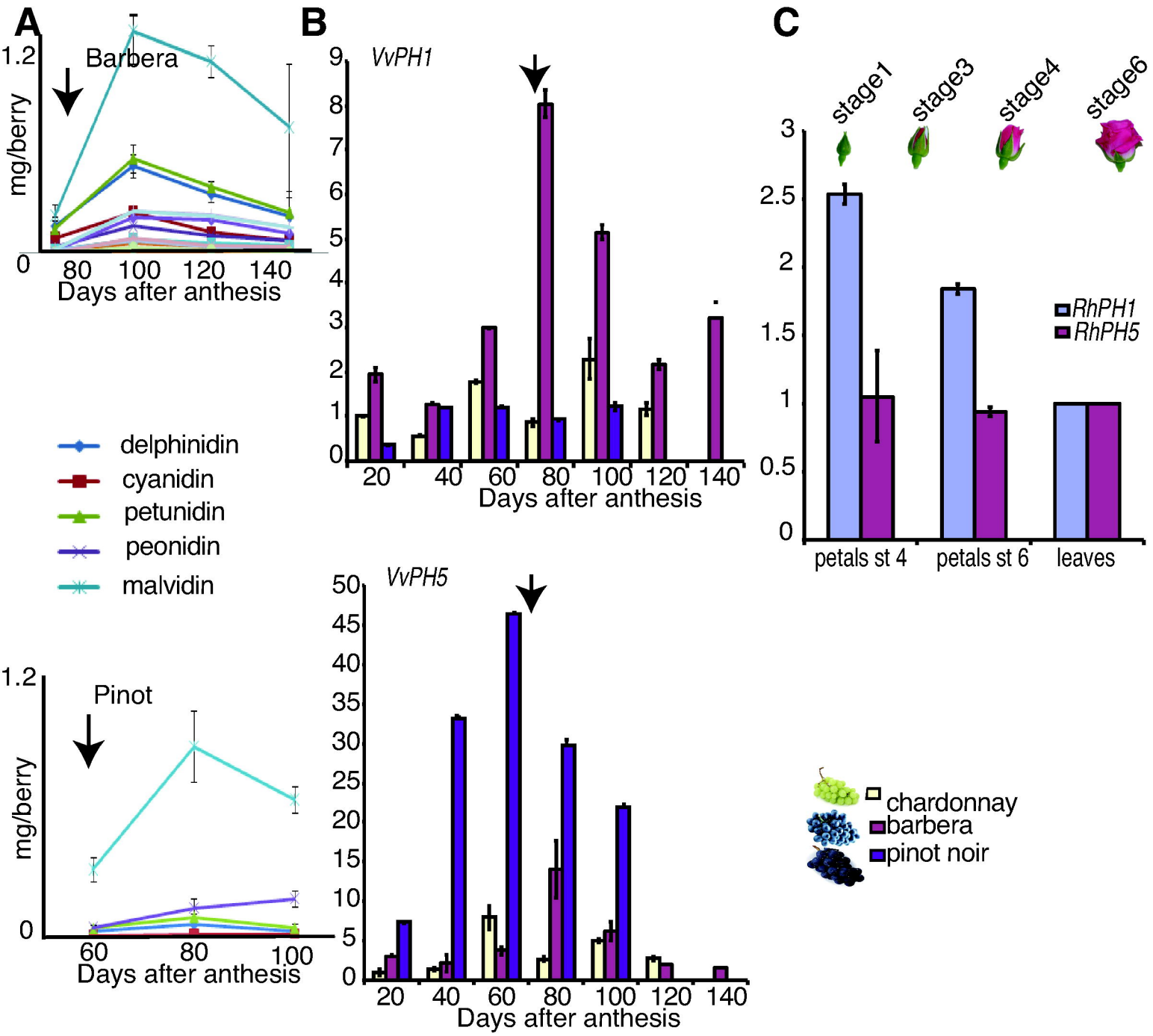

Figure 11. RT-PCR analysis of the expression of rose and grape homologs of PH1 and PH5.

(**A**) Accumulation of anthocyanin pigments during development of Barbera en Pinot berries. In Barbera veraison (arrow) occurs two weeks later than in the other two varieties.

(**B**) Relative expression of Vv PH1 and Vv PH5 in developing chardonay, pinot and barbera berries. The arrow indicates véraison. Expression in berries of Chardonnay 20 days after anthesis has been chosen as reference.

(**C**) Expression of Rh PH1 and Rh PH5 in the last stages of the development of the flower buds and in the leaves of rose.